AD-A135 878 CHARACTERISTICS OF AN INTEGRATED OPTICS RING RESONATOR 1/1
(U) UNIVERSITY OF SOUTHERN CALIFORNIA LOS ANGELES
CENTER FOR LASER STUDIES E GARMIRE AUG 83
UNCLASSIFIED AFOSR-TR-83-1048 AFOSR-82-0098 F/G 20/6 NL

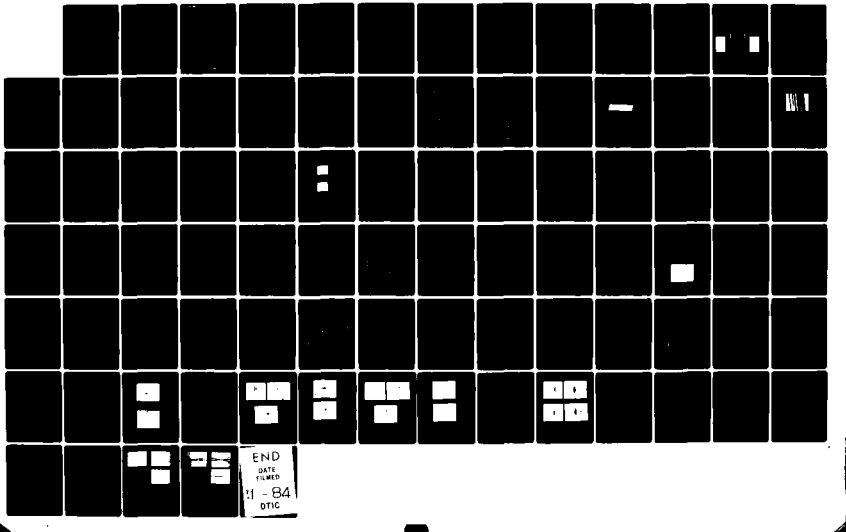

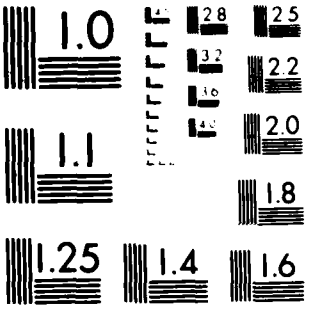

UNCLASSIFIED

SECURITY CLASSIFICATION OF THIS PAGE (When Data Entered)

(14)

AD-A135878

REPORT DOCUMENTATION PAGE		READ INSTRUCTIONS BEFORE COMPLETING FORM
1. REPORT NUMBER AFOSR-TR- 83-1048	2. GOVT ACCESSION NO. AD-A135878	3. RECIPIENT'S CATALOG NUMBER
4. TITLE (and Subtitle) Characteristics of an Integrated Optics Ring Resonator		5. TYPE OF REPORT & PERIOD COVERED Final Report May 1979-January 1983 6. PERFORMING ORG. REPORT NUMBER
7. AUTHOR(s) E. Garmire		8. CONTRACT OR GRANT NUMBER(s) AFOSR-82-0098
9. PERFORMING ORGANIZATION NAME AND ADDRESS Center for Laser Studies University of Southern California Los Angeles, CA 90089-1112		10. PROGRAM ELEMENT, PROJECT, TASK AREA & WORK UNIT NUMBERS 61102F 2305/B2
11. CONTROLLING OFFICE NAME AND ADDRESS AFOSR/NE Building 410 Bolling AFB, Washington DC 20332		12. REPORT DATE August 1983 13. NUMBER OF PAGES 82
14. MONITORING AGENCY NAME & ADDRESS(if different from Controlling Office)		15. SECURITY CLASS. (of this report) UNCLASSIFIED 15a. DECLASSIFICATION/DOWNGRADING SCHEDULE

16. DISTRIBUTION STATEMENT (of this Report)

Approved for Public Release; Distribution Unlimited

17. DISTRIBUTION STATEMENT (of the abstract entered in Block 20, if different from Report)

18. SUPPLEMENTARY NOTES

DTIC ELECTE DEC 15 1983 D

19. KEY WORDS (Continue on reverse side if necessary and identify by block number)

Integrated Optics
Waveguides
Resonator

20. ABSTRACT (Continue on reverse side if necessary and identify by block number)

A ring resonator 4 cm in diameter was fabricated and tested for sensing applications. A finesse of four was measured, and agreed with measured coupling efficiency and losses. Techniques have been developed to reduce the loss and from our measurements we predict that a finesse of more than 20 should be easily achievable in an interferometer 4 cm in diameter. This device has a wide variety of applications from temperature and wave-

DD FORM 1 JAN 73 1473

UNCLASSIFIED

SECURITY CLASSIFICATION OF THIS PAGE (When Data Entered)

DTIC FILE COPY

20. (Cont'd)

length sensing to inertial rotation sensing.

Further refinements which will produce a high finesse resonator are the fabrication of a single mode ring and using specially prepared optical glass substrates. Operation at wavelengths longer than 0.63 μm will also improve the performance.

TABLE OF CONTENTS

I. INTRODUCTION AND SUMMARY

This contract was for research and development of a ring resonator for sensing applications. This program was driven by the possibilities of passive ring resonator approach to inertial rotation sensing. The resonator consists of an integrated optics ring fabricated in glass with as large a diameter as possible. Coupling onto and off of the resonant ring is provided by directional couplers, straight-channel waveguides in close proximity to the ring. Such a ring has applications not only for inertial rotation sensing, but also for other sensing applications, such as temperature, acoustics, and wavelength.

During the first part of this four year research period we studied loss mechanisms in glass waveguides. We were able to develop techniques to reduce the loss to less than 0.1 dB/cm, adequate for high finesse ring resonators. We also developed the process of laser writing, in order to obtain large diameter masks suitable for ring resonator applications. Finally, we fabricated and characterized a ring resonator, determining that its properties agreed with design calculations. The contract was over before we were able to fabricate a ring resonator with a single mode waveguide on low-loss sbustrates. We predict, however, on the basis of this program, that high finesse large-diameter resonatorsin glass are indeed possible, and will have applications to inertial rotation sensing, high resolution wavelength measurements, and other measurements such as temperature and acoustics. Our preliminary research indicates that further development is needed to fulfill the potential of the glass ring resonator.

A. Outline of report

This report is divided into sections describing each of the research areas investigated during the course of this project.

Section II describes the characteristics of the ring resonator itself. These results were published in SPIE proceedings, and are currently being prepared for more complete publication in the Journal of Lightwave Technology. We made three ring resonators 4 cm in diameter, each with approximately seven lateral modes in the waveguide, and each demonstrating resonance. The best

resonators showed finesses on the order of four with the signal superimposed on a non-resonant background occuring from the multimode character of the waveguides and/or from depolarization which was later measured. The measured finesse agreed with the calculated finesse based on measured losses and coupling efficiencies in the directional couplers. Design calculations show that finesses on the order of 20 should be obtainable using the techniques developed in this contract.

Section III gives details of a measured depolarization occurring in waveguides with uneven walls. Such depolarization causes a large nonresonant background in the ring resonator and must be understood and eliminated before the resonator is fully optimized. We have proven that the depolarization is due to edge roughness in the mask and can be reduced considerably by using good quality masks. TM modes were shown to have considerably less depolarization than TE modes, although sufficient that it was typically 6% per centimeter. Since the ring resonator is roughly 12 cm long, this small depolarization becomes large in the resonator - typically between 25 and 50%. Further research is required to determine the fabrication-dependence of such depolarization. We are currently writing these results up for publication and would like to continue research in this area.

Section IV describes the directional couplers used in the ring resonator, explaining why only the highest order mode was coupled out of the ring resonator. Good agreement was seen between measured coupling efficiencies and theoretical modelling.

Section V describes our waveguide fabrication techniques and shows the refractive index profiles obtained under different conditions. Recent emphasis has been placed on ion exchange with KNO_3 into specially prepared soda-lime glass. These results will be published in the Journal of Lightwave Technology.

Section VI describes our extensive research into the losses in glass waveguides, some of which have been published in Applied Physics Letters, others in SPIE proceedings and still more are in manuscript form at the present time. We show that using Schott S3 glass, speciallly prepared without fining agents, three-mode

planar waveguides can be fabricated with losses the order of 0.1 dB/cm at 0.63 μm. We show, furthermore, that losses are less both for longer wavelengths and for waveguides buried below the surface. Finally, we show that channel waveguides have roughly the same loss as planar waveguides. We therefore expect that losses approaching .01 dB/cm will be obtained at 1.3 μm.

Section VII lists references which are useful to understanding aspects of the ring resonator referred to in this report.

Section VIII contains a list of publications, presentations, contacts with industry, government and universities, and a list of personnel involved in the program. Section IX contains selected reprints on losses in glass waveguides and on laser writing.

B. Additional Research Required

The concept of the large-diameter ring resonator in glass has been demonstrated. However, there are some further developments required to achieve optimum performance.

First, the resonator must be fabricated on S3* glass, which we have demonstrated has suitably low loss, to increase the finesse. Second, the directional coupling efficiency onto and off of the ring must be reduced. This can be achieved by using a shorter fabrication time, resulting in waveguides which are not so deep or wide. Finally, operation at longer wavelengths must be demonstrated. We expect to achieve a single mode ring at 1.3 μm with the ring mask we currently have available. We also expect that both the losses and directional coupling efficiencies will be less at these longer wavelengths. We expect that finesses approaching 20 can be demonstrated using our laser-written mask.

In a parallel effort, a new mask must be obtained which has narrower channel waveguides and more symmetric directional couplers. We are prepared to make this mask by laser writing. In addition, comparison with commercially obtained masks should be made, to determine which has the least edge roughness.

There are three research areas remaining as an outgrowth of our pioneering experiments. First, we need to characterize, quantify and eliminate the depolarization we have discovered. Second, we need to refute, or confirm, possible evidence of a degredation of ion-exchanged waveguides with time. This latter effect, if true, will mean that alternative fabrication techniques such as field-assisted diffusion in which we observed no degredation, should be used. Finally, we need to develop ion-exchange techniques

to bury the waveguide below the surface and further reduce its loss.

C. Ring Resonator Device Considerations

We have measured a finesse of 4 in a ring 12 cm in circumference. Given the ability to detect the center of the line of 10% of its width, the experimental resonator can be used to sense changes of 1/40 of its interorder spacing. Consider that a temperature change causes a length change with a coefficient of linear expansion of glass of about 10^{-5}/°C. Thus a circumference of 12.5 cm will increase by 1.25 μm/°C, or roughly three wavelengths (measured in the medium) per degree. Since 1/40 of a wavelength can be resolved, a temperature change of .01°C can be measured. Correspondingly, a frequency change of 5×10^{-4} Å can be measured, resulting in a fringe shift of 1/40 of an interorder spacing.

When we build a resonator with finesse 20, the center of the resonance can be easily determined to 1/200 of the interorder spacing, and the sentivity to temperature and frequency shifts will be five times larger. That is, .002°C and 1×10^{-4} Å respectively, can be measured. With somewhat more sophisticated signal processing techniques, ten times greater sensitivity should be achievable.

For inertial rotation sensing, the passive ring gyro will require higher finesse and more sensitive methods of measurement to approach the performance of the fiber gyro. Assuming, as above, that the center of the resonance can be determined to 1/200 of the interorder spacing, the ring resonator should be able to sense 188°/sec rotation. This is determined from the Sagnac effect:

$$\Delta L = (4A/c)\Omega \ ,$$

where A is the area enclosed by the ring, and c is the velocity of light in vacuum and Ω is the angular rotation rate. By increasing the finesse to 200, (eliminating residual losses and reducing the coupling efficiency onto and off of the ring) and by improving the sensing techniques so that the center of the resonance peak can be determined to one part in 10^3, the sensitivity can be improved to measure 0.2°/sec. This approaches the sensitivity of the fiber gyro reported by McDonnell Douglas, and would be a convenient integrated optics device.

Optimization of the size of the ring resonator is determined by the loss per unit length. In the limit in which the linear loss dominates the finesse, it may be given approximately by $F = (\alpha r)^{-1}$. The 1/r dependence cancels one power of the radius dependence in the rotation angle, and we find that the sensitivity is proportional to the diameter of the ring, not its area. In particular, when the losses are .01 dB/cm, $\alpha = .0023\ cm^{-1}$, and for r = 2 cm, $F \rightarrow 217$. Since we have shown that, in principle, the losses may approach .01 dB/cm, then F = 200 and rotation rate sensitivities of 0.2°/sec will be obtainable.

It must be noted, however, that extremely stable laser sources must be used with this resonator in inertial rotation sensing. Conversely, the ring provides an excellent means of measuring the wavelength of lasers which are not stable in frequency. This makes the integrated optics ring resonator into a wave-meter. It has advantages over conventional Fabry-Perot interferometers because there is no retro-reflected signal. Such a convenient wavelength sensor can also be used in wavelength stabilization feedback schemes for dye lasers or semiconductor lasers.

II. RING RESONATOR

In this section we describe our results on the first large-diameter resonators ever made in glass waveguides. This work was first reported at SPIE in Washington in May.

A. Summary of Results

The geometry we use is shown in Figure II-1, and consists of a ring waveguide approximately 20 μm wide with directional couplers onto and off of the ring. The mask used to define the channel waveguides was fabricated in our laboratory by Laser Writing. Difficulties in fabrication of the mask used for the ring reported here caused the width of the ring channel to vary from a minimum of 15 μm to a maximum of 25 μm. The directional couplers which couple light onto and off of the ring are shown in Figure 1, and are seen to have a separation of 51 and 12 μm, measured from inner edge to inner edge, at the closest spacing. The varying width of the ring waveguide introduces mode mixing and can be corrected in the future using a better mask. The fact that the two waveguides in the directional coupler are not identical is not a serious problem, however, because only a small percentage of coupling is desirable to achieve a high finesse resonator. The coupling coefficient measured in the experiments reported here was larger than optimal, and increased waveguide channel spacing would be advantageous and would increase the resonator finesse.

The waveguides were fabricated by ion exchange from a KNO_3 melt at 400°C. Channel definition was accomplished by coating glass substrates with 2000 - 4000 Å aluminum as a mask against ion exchange. Channels defining the optical circuit were opened in the aluminum using photolithography and chemical etching. Ion exchange for between 2 and 4 hours resulted in waveguides which contained two or three out-of-plane modes and five to seven in-plane modes. From determinations of the index profile using the WKB method on planar waveguides, we estimate that the thickness of the waveguide was between 3 and 5 μm. The substrates were Eastman Kodak Lustra Glass,

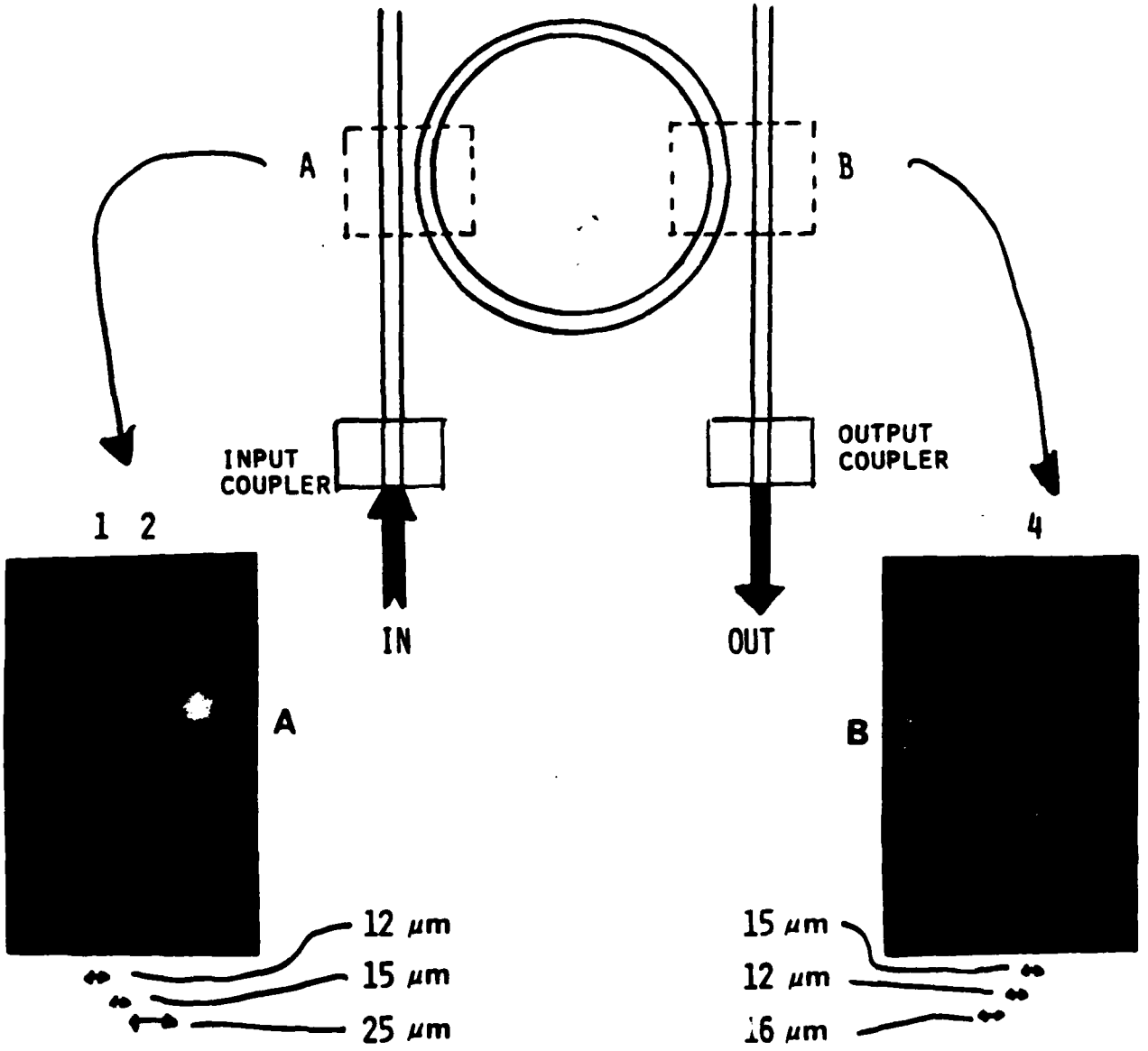

Figure II-1. Mask and measurement apparatus for integrated optics ring resonator showing dimensions and the directional coupling region.

which are a convenient source of flat soda lime silicate glass of the proper dimensions. Experiments to measure the losses in planar waveguides in similar glass showed losses the order of 0.5 dB/cm.

Three ring resonators were tested, and the results of ring No. 3 are shown in Figure II-2. The resonators were driven through their resonances by heating. Excitation was with a single frequency HeNe laser. The curves are the transmission as a function of time, as the interferometer slowly cools. Several features are noted in these curves. First, there is a large amount of background light which does not have resonance behavior. This may be due to intermodal scattering within the ring, which will be discussed below. Secondly, the slow increase in the period with time is caused by a nonuniform cooling rate. Third, the slow drift in intensity is caused by changes in input prism coupling with temperature and would be eliminated with end-fire coupling and lastly, the finesse is under four, due primarily to waveguide loss.

The dependence of resonator finesse on waveguide loss can be seen from the expression for the transmission of the ring resonator, which is given by

$$T_r = \frac{T}{(1-R)^2 + 4R \sin^2 \phi} \tag{1}$$

with T and R given by

$$T = K_{12}K_{34}\exp(-\pi\alpha r) \tag{2}$$

and

$$R = (1-K_{21})^{\frac{1}{2}} (1-K_{34})^{\frac{1}{2}} \exp(-\pi\alpha r) \tag{3}$$

where K_{ij} is the power coupling efficiency from the ith to the jth waveguide (defined numerically as shown in Figure 1), α is the loss per unit length, r is the radius of the ring and ϕ is the round-trip phase change for light in the ring. The fact that the guides were multimode and nonidentical results in $K_{ij} \neq K_{ji}$.

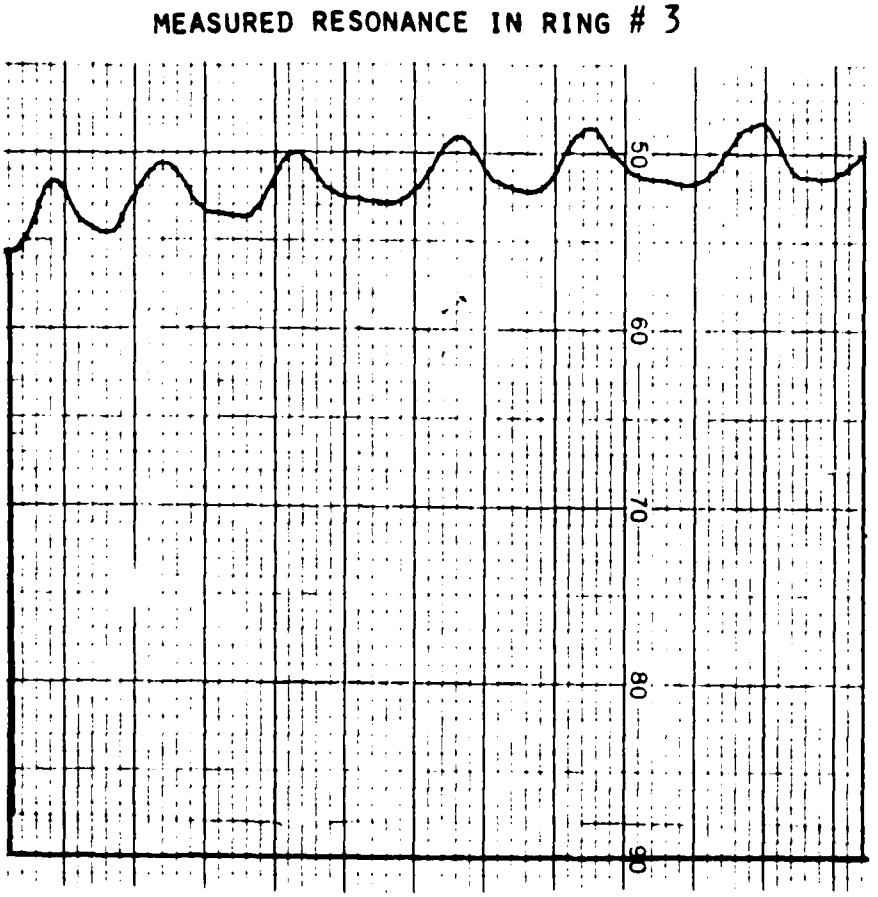

Figure II-2. Measured resonance in ring No. 3, determined from the transmission as a function of time while the device is cooling.

Careful measurements of the coupling coeffients were made for devices with two different fabrication conditions and are shown in Table II-1. It should be noticed that decreased diffusion time causes a decrease in the coupling coefficients, presumably since there is less ion exchange under the mask. Even allowing for ion exchange under the mask, the closest approach of the inner edges of the two waveguides is 5 μm. In numerical simulations of the directional coupler, we observed that there is negligible coupling of low order modes when waveguides are spaced as far as 5 μm. However, higher order modes will have larger coupling coefficients and produce measurable coupling between the two waveguides.

Photographs of the mode pattern prism-coupled from the output arm of the interferometer show that the light is in the m = 6 in-plane mode, when the resonator is both on resonance, and off resonance. Furthermore, there is only one mode in the direction transverse to the plane of the ring. Photographs of the modes prism-coupled from the ring, however, show that all three modes transverse to the plane were coupled from the input arm onto the ring. Of these modes, only one is directionally coupled off into the output arm.

The fact that only the highest order mode is coupled out of the ring makes it possible to see resonances in the resonator even in the presence of a large number of other modes. However, the presence of other modes in the ring is probably responsible for the large amount of background nonresonant light. This may occur because of mode-mixing due to scattering within the ring. Such scattering can be seen in the m-lines from planar waveguides. This means that although light of several modes was excited into the ring, much of this light scatters into the highest order mode, travels around the ring, and couples out in a nonresonant fashion.

The expected model for the transmission function of the ring, in the presence of a nonresonant background is

$$T = T_r + T_b \tag{4}$$

where T_r was described in equation 1 and T_b is the background

TABLE II-1. PARAMETERS OF MEASURED RESONATOR

RING #	MEASURED FINESSE	K_{12} %	K_{21} %	K_{34} %	K_{43} %	ION EXCHANGE TIME (HOURS)	LOSS DB/CM
2	2.2	15	25	54	16	4	1.23
				49	18		
3	3	ASSUMED SAME AS #2				4	0.6
4	4	6	16	33	14	2½	0.4
			21	32	10		

level.

The finesse is defined as the ratio of the width of the resonance, T_r to the interorder spacing, independent of the background level. The finesse can be expressed in terms of the reflectivity of the resonator as

$$F = \pi \left(2\sin^{-1} \sqrt{\frac{(1-R)^2}{2(1+R^2)}} \right)^{-1} . \qquad (5)$$

This may be inverted to give the reflectivity in terms of the finesse:

$$R = \frac{1 - \sin(\pi/F)}{\cos(\pi/F)} . \qquad (6)$$

From a determination of the reflectivity R and measurement of the coupling coefficients K_{ij}, we determine the loss per unit length through the expression

$$\alpha = - \frac{1}{\pi r} \ln \left[\frac{R}{\sqrt{1-K_{21}}\ \sqrt{1-K_{34}}} \right] \ \text{cm}^{-1} . \qquad (7)$$

In terms of dB/cm, the loss is $\ell = 4.3\alpha$.
Losses calculated by this method are shown in Table II-1. The loss calculated for ring No. 2 is high because there was a break in the ring caused by incomplete removal of the aluminum mask in the waveguide channel before ion exchange. The losses measured in the other two rings are comparable to that measured in planar waveguides fabricated in similar glass by the same techniques. The longer diffusion time causes more ion exchange and a higher value of Δn at the surface, which causes more intermodal scattering and somewhat higher loss.

Attempts to measure the loss in the ring directly by comparing intensities of light coupled out with a moving prism led to much higher values of measured loss, on the order of 1.4 db/cm. However, after this measurement was made, the ring no longer showed any resonance behavior, suggesting that surface deformations caused by placing the prism directly on the ring caused

irreversible damage and an anomalously high measured value for the loss in the channel. Measurements of the finesse offer the most accurate determination of loss, here about 0.5 dB/cm.

The ring we have fabricated will have fewer modes if it is used at longer wavelengths. To understand the wavelength-dependence of the guides, we model the transverse modes as those of a planar waveguide of inverse hyperbolic cosine square profile. In this case, the number of modes at cutoff is given by

$$2M + 1 \leq \sqrt{1 + V^2} \text{ where } V = \frac{2\pi}{\lambda} d \sqrt{2n\Delta n} \qquad (8)$$

Since light at 0.63 μm wavelength propagates in 7 modes in a waveguide of width 12 μm, the V parameter is 15 and the index increase inside the waveguide is $\Delta n = .0052$. If the wavelength is increased to 0.83 or 1.3 μm, the number of modes is decreased to 5 and 2, respectively. Reduction of diffusion time will reduce the number of modes still further, and fewer modes should reduce the measured nonresonant background.

The use of longer wavelengths has also been shown to reduce the loss in waveguides by typically a factor of three. In addition, losses of less than 0.1 dB/cm at 0.63 μm have been measured in planar waveguides fabricated in Schott S3 soda-lime-silicate glass which was specially prepared without fining agents. Finally, burying the waveguide below the surface will reduce the loss even further. In figure II-3 we show the results of a calculation predicting the finesse of several values of waveguide loss and coupling coefficients. We see that a finesse of 16 should be measured if the loss is reduced to 0.1 dB/cm and the directional coupling coefficients reduced to 5%.

The resonances which we measured were produced by heating the waveguide. The temperature dependence of the optical path length in glass is given primarily by the expansion of the material; the coefficient of linear expansion of glass is about 10^{-5}/°C. Since the light travels about 2×10^5 wavelengths in the ring, a change in temperature of 1°C should

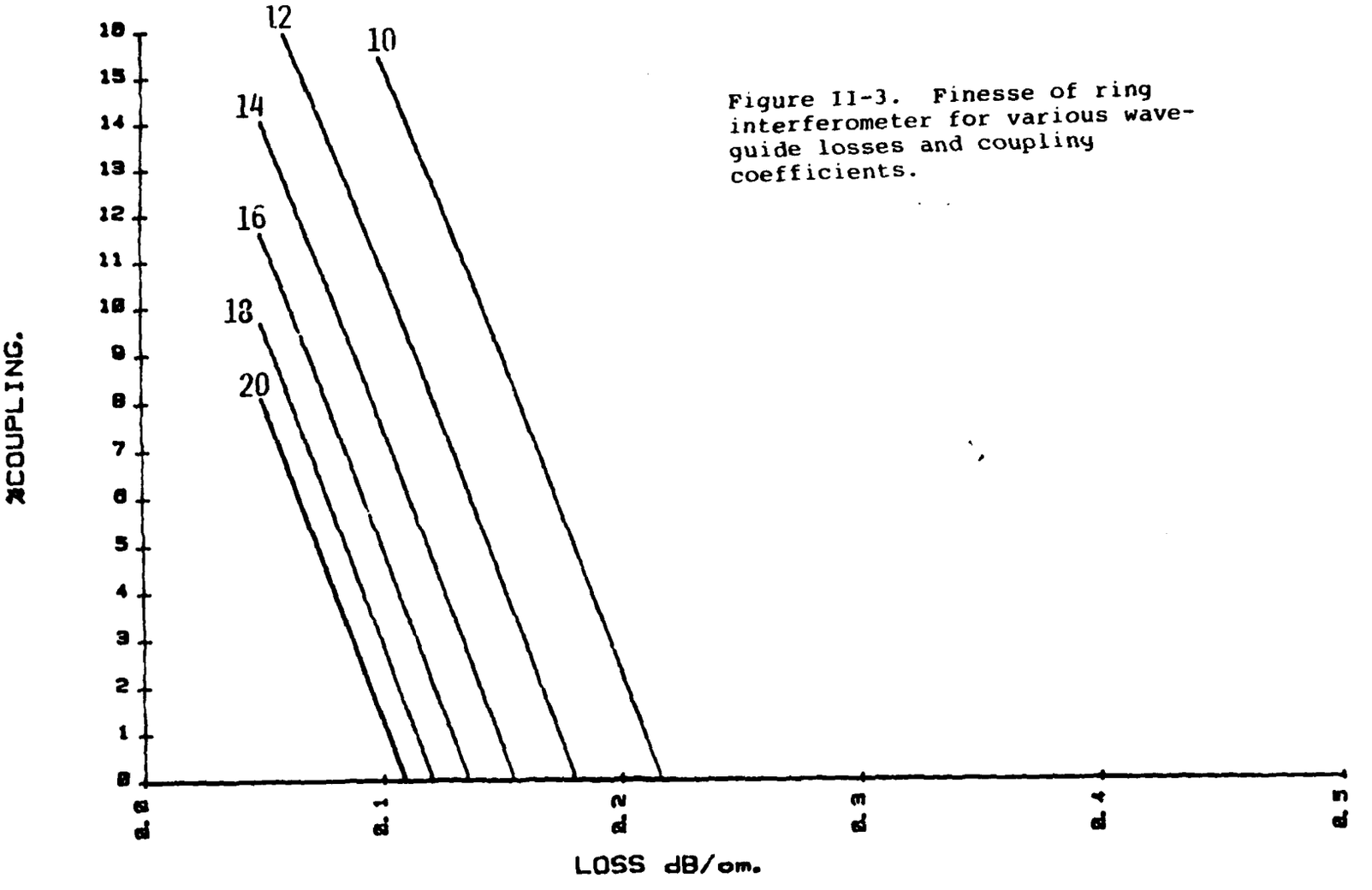

Figure II-3. Finesse of ring interferometer for various waveguide losses and coupling coefficients.

cause the resonator to track through two resonances. This gives a measure of the sensitivity of the ring. Even with the poor finesse in the device we have published here, we can find the peak to about 20% of an order, so that temperature changes on the order of 0.1°C should be measurable with this ring. Increasing the finesse a factor of five will increase the sensitivity a factor of five. However, the use of the ring as a temperature sensor requires a stable laser input.

Conversely, the ring may be used to monitor frequency shifts in a laser. The wavelength monochromaticity required by a resonator is given by $\delta\lambda = \Delta\lambda/F$ where $\Delta\lambda$ is the free spectral range of the interferometer = $\lambda^2/2\pi nr$. This corresponds to a frequency stability of 5×10^{-3} Å, required to stay on resonance for a resonator with finesse = 4. This means that this resonator is an excellent means for measuring drift in lasers which have a tendency to drift in frequency. It may also be used in connection with feedback correction to stabilize the laser output. This may find application with narrow linewidth semiconductor lasers.

A particular advantage of the ring resonator over a Fabry-Perot is the fact that off resonance the light is not reflected back toward the source but continues out the input channel, thus causing no interference with the source.

B. Additional Considerations

In this section we present several items of data on the ring resonator which were not reported at SPIE.

First, Figure II-4 shows the resonator transmission for ring No. 3 when two modes are excited. We have superimposed with dashed lines two traces with the finesse shown in Figure II-2, which can be seen to explain the experimental trace. Clearly it is required that only one mode be coupled out of the resonator if the highest resolution is to be measured. The variable spacing results from a nonuniform cooling rate.

For comparison, single-mode traces of resonators Nos. 2 and 4 are shown in Figure II-5. The poor finesse of No. 2, which

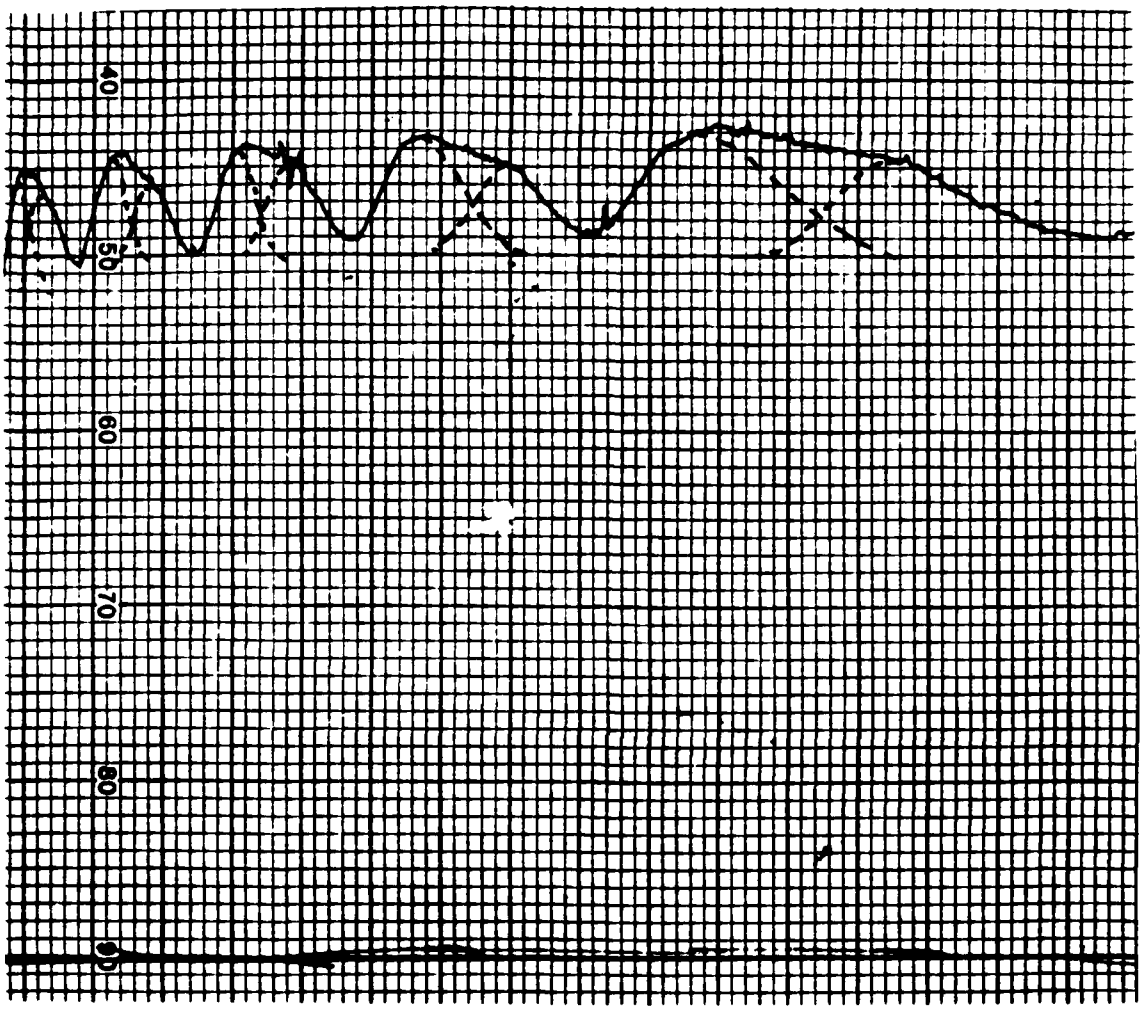

Figure II-4 Interferogram of ring #3 with two modes excited. Dashed lines represent two modes which are superimposed in the output. The nonuniformity of the trace is due to non-uniform cooling of resonator.

Fig. II-5 Interferograms of two other ring resonators

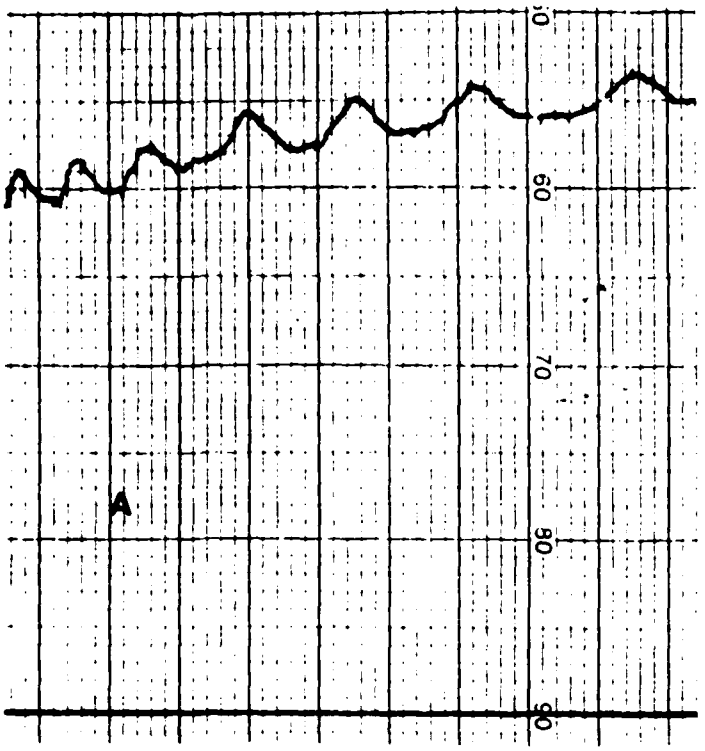

A) Ring #4, showing a finesse of 4

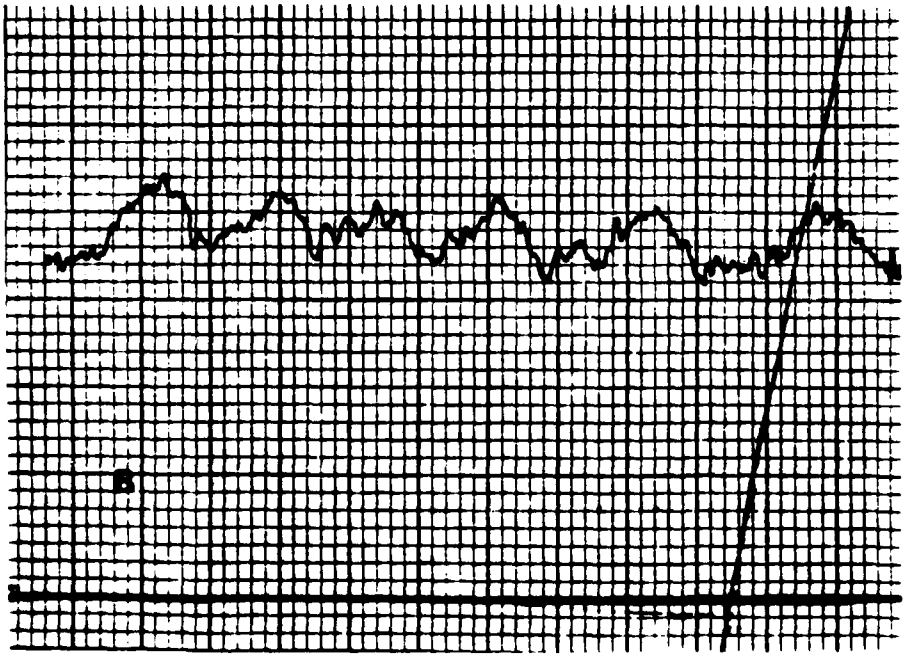

B) Ring #2, showing a poor finesse due to excess loss in the ring.

had unusually high loss is evident, along with the higher finesse of No. 4.

The guides of the resonator were typically highly multi-mode, but only one mode was typically coupled into the output channel. The largest coupling coefficient occurs for the highest order mode. Proof that only the highest order mode was coupled out of the ring was provided by a photograph of the far-field of the guided wave in the output channel. This is shown in Fig. II-6 and demonstrates the seven-lobed output of higher-order mode.

A lossy ring resonator can be used as a channel-dropping filter , without the need for the output arm. We did not measure this property of our ring resonators and it remains an area to be investigated in the future.

Several effects came up in the study of these resonators which we were not able to fully pursue. Further research is required to illucidate the reasons for these effects.

First, we observed a depolarization of light travelling within the channel waveguides, both straight and curved. This depolarization was not known when the preliminary measurements on resonator finesse were completed, so it is not known how much of the background measured in the output was due to depolarization effects. A later section discusses depolarization in more detail.

Second, we found that after a period of time the ring resonator no longer showed resonance fringes. In ring No. 2 we believe this was due to pressure on the surface of the waveguide from the prism introducing additional loss and destroying the finesse. In the other rings, we postulate that operating them at elevated temperatures during the heating to measure resonance may have caused diffusion of sodium. Indeed, eventually these samples no longer acted as waveguides. The temperature range over which these devices may be safely operated remains a problem for further study.

Figure II-6 . Output channel of ring interferometer. Far field of the output of a prism coupler.

Several experiments were performed to specifically look for degradation, although definitive experiments could not be completed by the end of the contract. For example, ring number 4 was kept in a clean room and out of the presence of light (except for safelights). Prism coupling indicated that the signal transmitted through the ring resonator was five times weaker after a month than its original value. The number of modes in the output was approximately the same as previously, although perhaps there was one less mode.

Not only the output of the resonator was much less than originally, the output of the straight channel was also less. Thus either prism coupling was not as effective, or the waveguide was much more lossy. Further experiments must be undertaken to identify whether this is a real problem.

Similar indications of possible degradation were also seen in planar waveguides. For example, in microscope slides, immediately after ion exchange in KNO_3 for 30 minutes, we observed a single mode. However, after approximately one month, we observed two modes, separated by approximately .005 rad. We are not sure, however, whether this is a real increase in the number of modes, or an improvement in our ability to measure weak modes. Degradation has been suspected in ion exchange waveguides in $LiNbO_3$ also. We propose a continuing investigation to decide whether or not degradation exists.

We were not able to complete fabricating a single mode ring resonator before the end of the program. It remains a subject of great interest to study the behavior of such a resonator, as well as to determine its stability.

III. DEPOLARIZATION OF LIGHT IN CHANNEL WAVEGUIDES

The large non-resonant background in the output of the ring interferometer caused us to question the possible depolarization of light in the waveguides. We made a series of measurements and did, indeed, find sizeable depolarization. In this section we describe experiments we made to investigate depolarization, and discuss the theoretical aspects.

A. Mode-conversion in Wide Channel Waveguides with Fixed Edge Roughness

In order to investigate the cause of mode-conversion, we made a mask which consisted of a single channel waveguide displaced and reprinted to produce wider channels with the same wall roughness. A photograph of one such pattern etched into aluminum before ion exchange is shown in Fig. III-1.

The measured mode-conversion is plotted as a function of waveguide width for waveguides between 30 and 150 um in width. Two different samples were fabricated and the data are shown in Figures III-2 to III-4. The first two are for two different samples, when the distance between the input and output coupling prism was approximately 3 mm. In Fig. III-4, this distance was 0.8 mm. In every case the depolarization is found to increase dramatically as the waveguide width narrows. Depolarization decreases to only about 1% by the time the waveguide is 150 um wide. Measurements on planar waveguides showed apparent depolarization of about 0.1%, while crossed polarizers transmitted only 0.02%. The signal measured with planar waveguides is attributed both to limits on alignment accuracy and to small amounts of scattered light.

In both samples, measurements at 3 mm showed comparable depolarization when the waveguide was excited with TE polarization. However, the depolarization of TM light differed dramatically in the two samples; in one case the depolarization is essentially polarization-independent, while in the other case the TE modes became depolarized at roughly twice the rate as TM modes.

In addition to depolarization, the waveguides experience mode conversion and loss which is a function of distance, since the mode

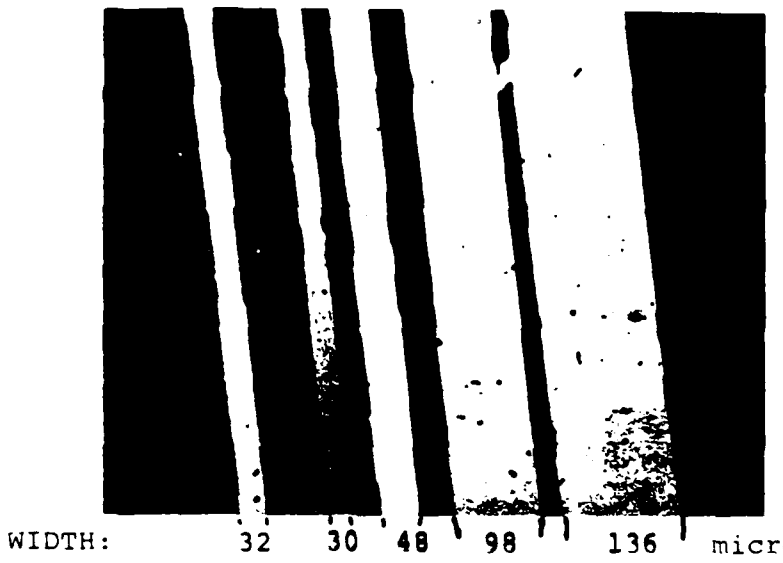

Figure III-1. Mask used to fabricate waveguides of fixed edge roughness and variable width

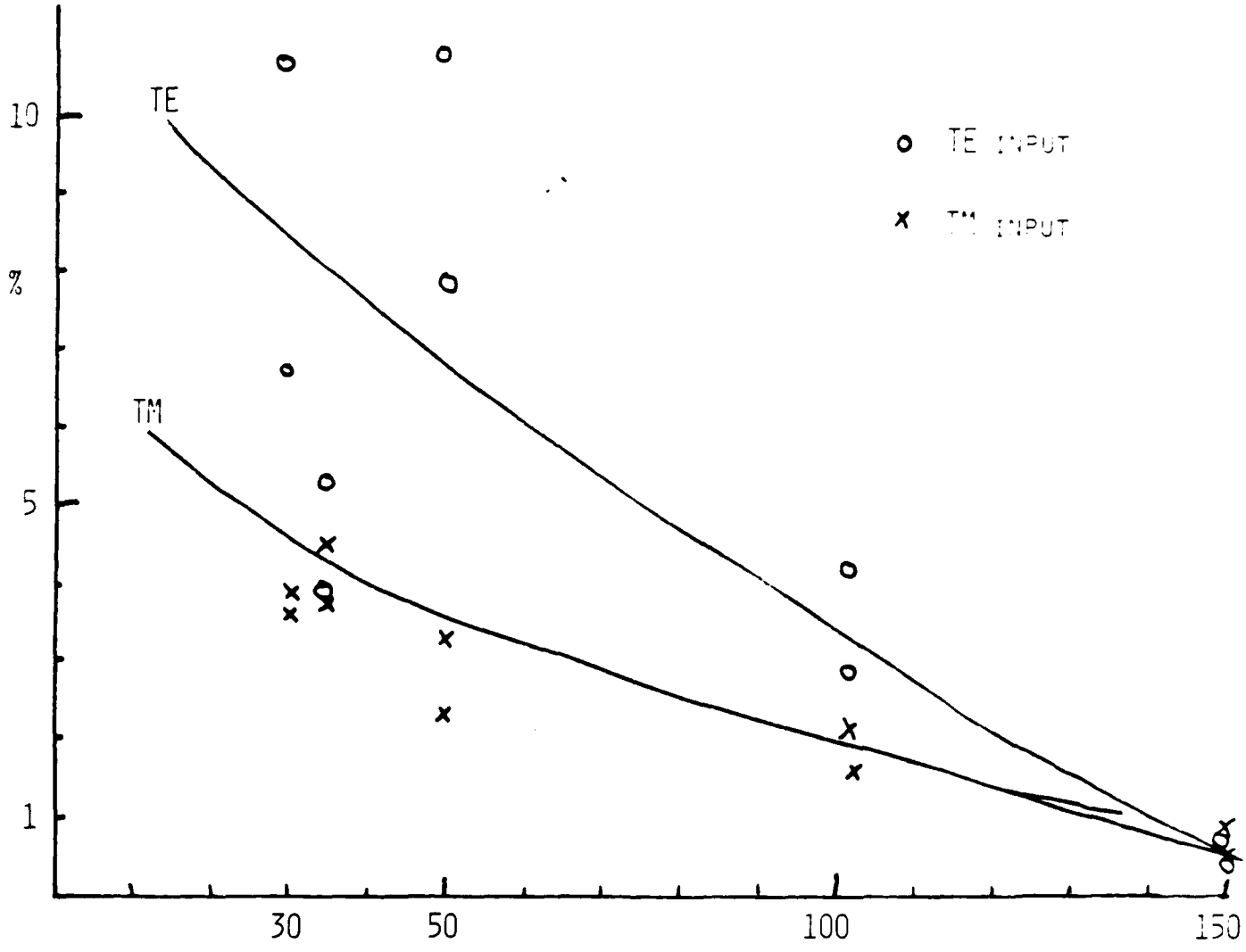

Fig. III-2. Depolarization as a function of waveguide width, sample 4. Measurements were made at a distance of 3.5 mm from the input coupler.

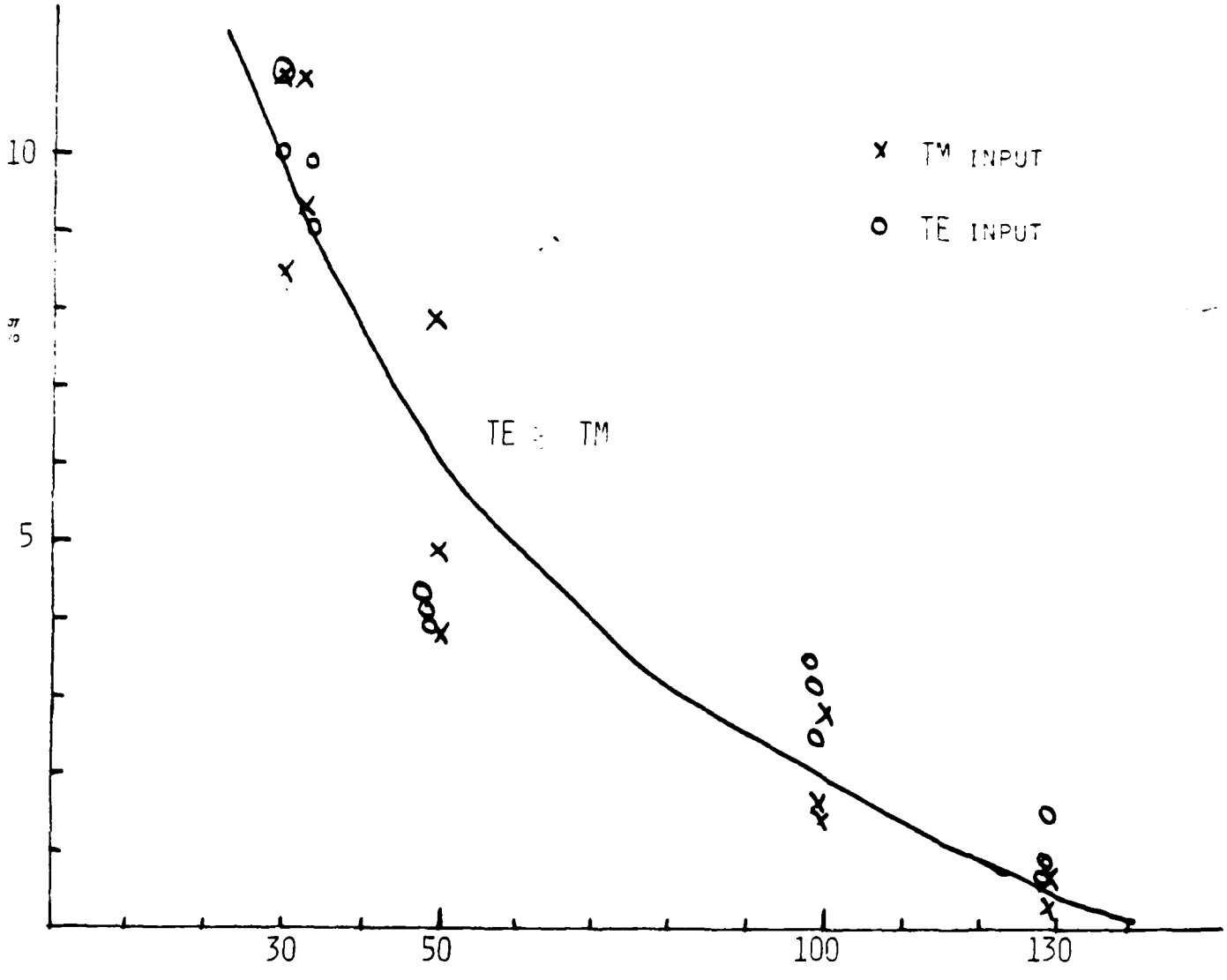

Figure III-3. Depolarization as a function of waveguide width, sample #5. Measurements were made at a distance of 3 mm from the input coupler.

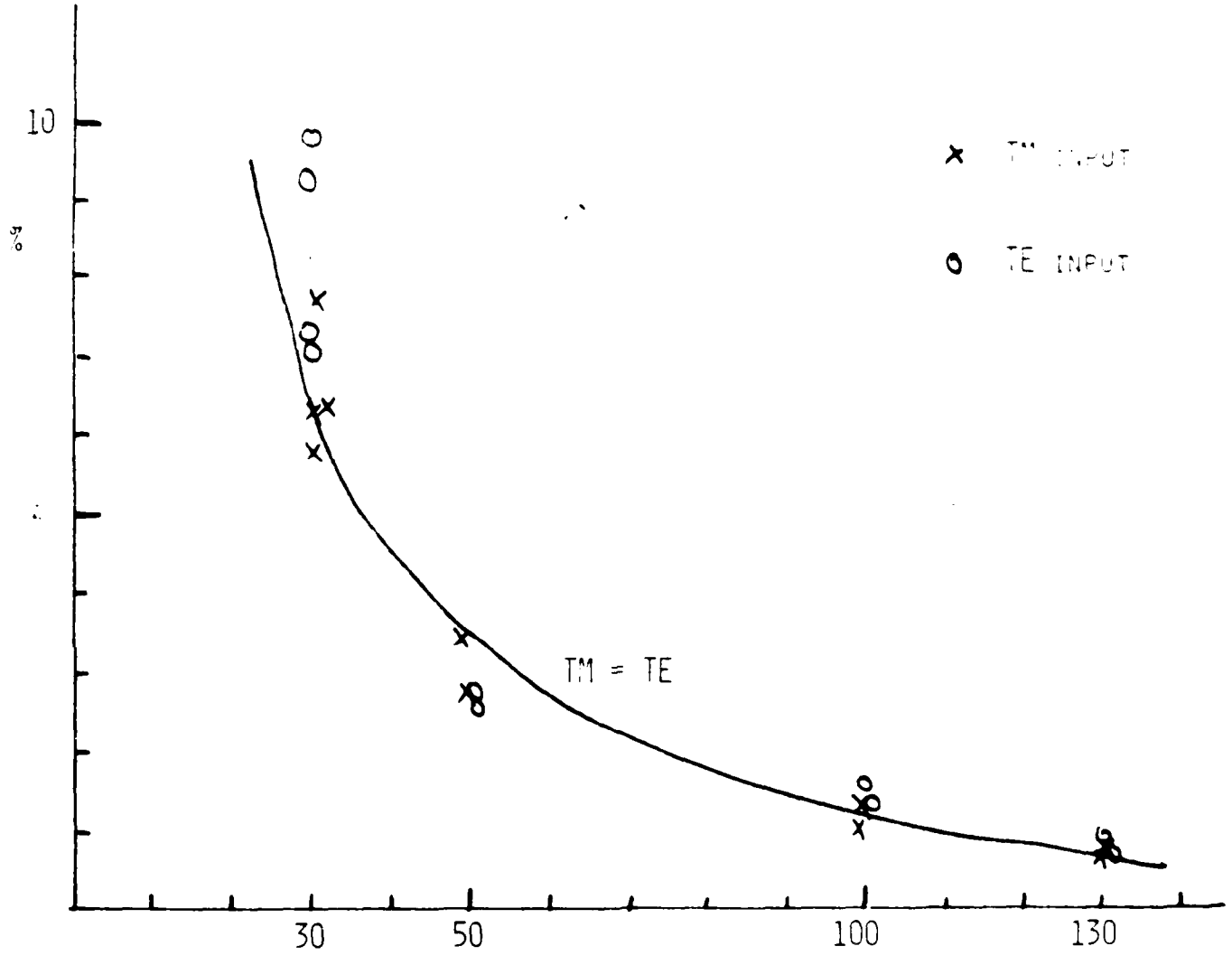

Figure III-4. Depolarization as a function of waveguide width, sample #5. Measurements were made at a distance of 0.8 mm from the input coupler.

content is a function of distance. In order to separate such effects from depolarization, we measured depolarization with as short a guiding length as possible: 0.8 mm. The results, shown in Fig. III-4, indicate similiar behavior to the results at 3 mm, although approximately half as much depolarization. This indicates that, for these samples, depolarization apparently was not linear with distance.

The question arises as to whether the depolarization occurs from the prism coupling process. We therefore prepared a sample and used endfire coupling to excite the modes. We monitored the polarization of the output both with endfire coupling and with prism coupling. In each case we saw depolarization comparable to that measured with prism coupling. Thus the depolarization does not occur in the prism. The fact that depolarization depends on the width of the channel indicates that it is probably due to waveguide roughness.

Since these waveguides were multi-mode, we attempted to measure the mode-dependence of the depolarization. The results were inconclusive. Table III-1 shows the results of depolarization in these waveguides. It was not possible to be specific about mode number, but to compare "low" with "high" order modes. The mode dependence of the depolarization can be seen by looking at the far field mode patterns for light coupled out of the guide with a prism. Fig. III-5 shows photographs indicating that the depolarized component has light only at the edges of the channel waveguide, in a higher order mode than the polarized component.

B. Depolarization in waveguides fabricated with a high quality mask

We obtained a mask which was much smoother, and fabricated 6 μm channels in an aluminum mask. By using shorter diffusion time we obtained single mode guides in depth. After ion exchange we saw that some waveguides retained the 6um width, while some other waveguides widened in an irregular fashion. We explained this by a local lifting of the aluminum mask during ion exchange. This process led to waveguide roughness and increased mode conversion.

Selecting the best waveguides, we plotted the percent depolarization as a function of distance for both TE and TM modes, shown in Fig. III-6. In this case the data could be fit to a linear length

TABLE III-1

MODE-DEPENDENCE OF PERCENT

DEPOLARIZATION IN CHANNEL WAVEGUIDES

WAVEGUIDE NUMBER	TM		TE	
	LOW ORDER MODES	HIGH ORDER MODES	LOW	HIGH
1	9.4%	20%	7%	12%
2	20	33		
3	17	13		
4	4	10		

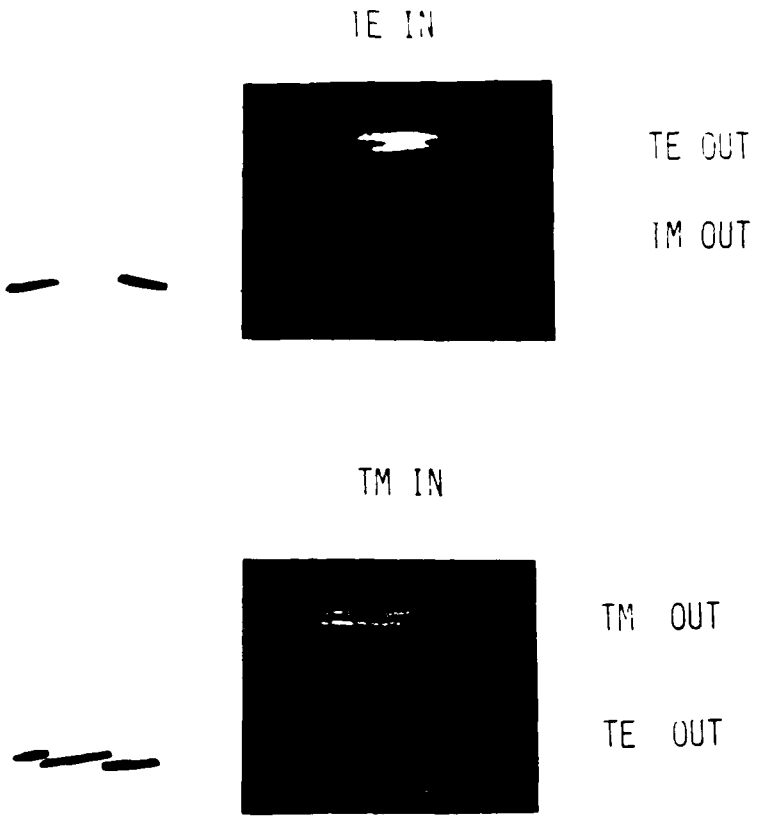

Figure III-5. Mode dependence of depolarized light. Upper pattern is the input polarization, showing two modes out of the coupling prism. Lower pattern is the depolarized component, showing a higher order transverse mode. A sketch of the depolarized component far field pattern is included for clarity.

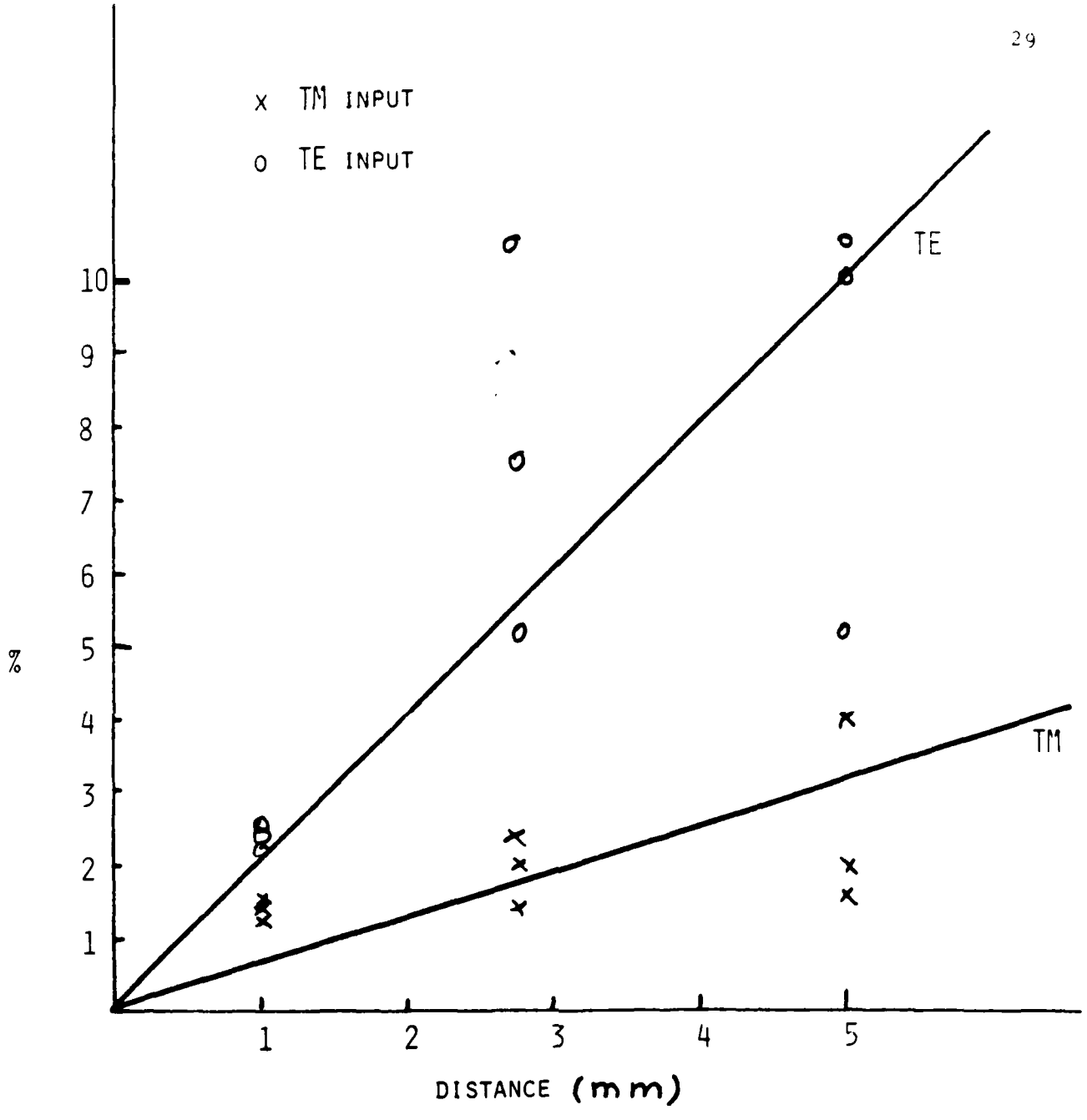

Figure III-6. Percent depolarization as a function of distance, for a good quality waveguide of 8 μm width (channels 5,6,7)

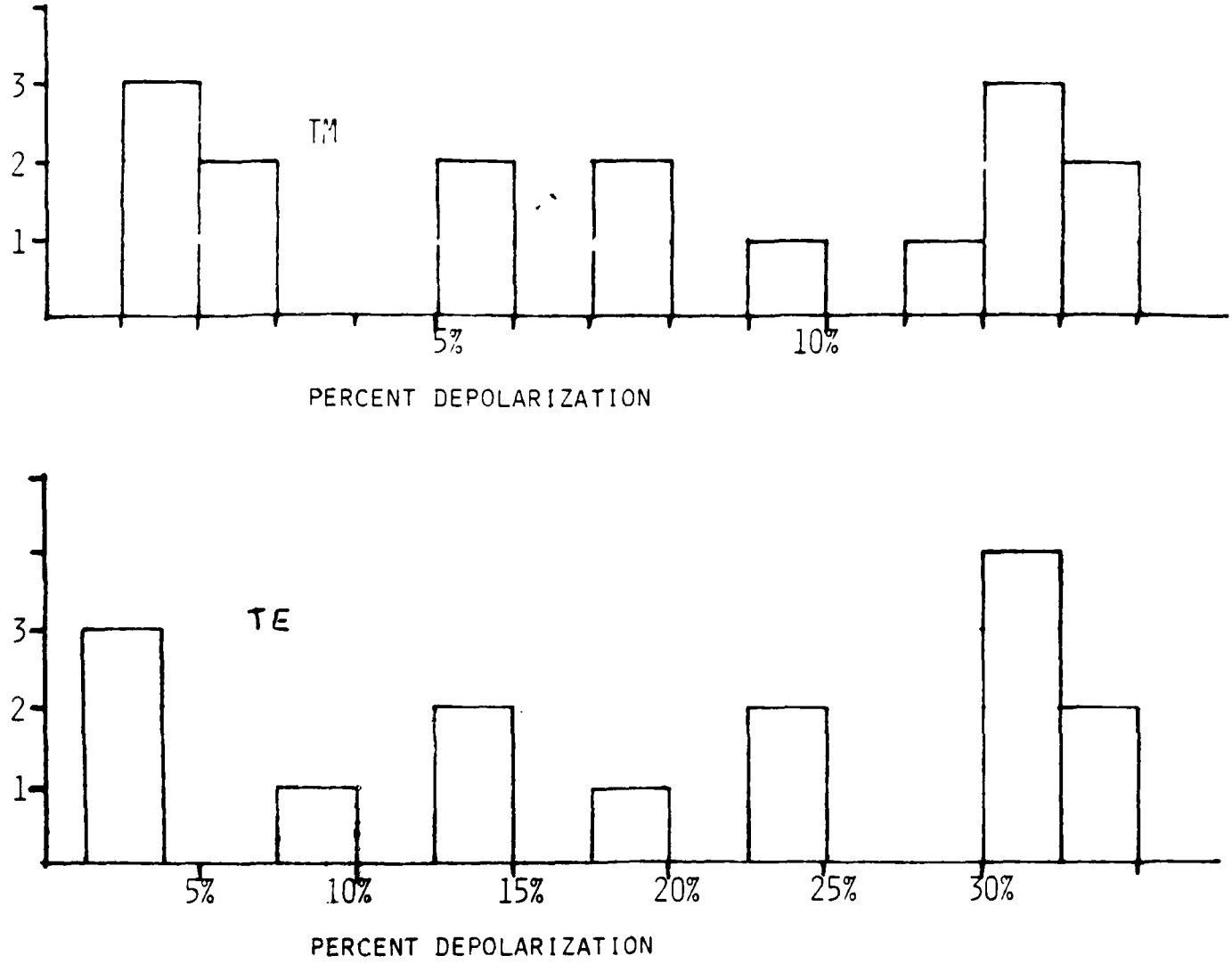

Figure III-7 Histogram giving number of channel waveguides with a given percent depolarization

dependence (the high value of depolarization for the TM mode at a distance of 1 mm is attributed to scattered light from the prism coupler). Furthermore, there is approximately two times more depolarization for TE modes than for TM modes. Figure III-7 shows a histogram of the number of waveguides obtained with a particular value of depolarization at a coupling length of 1 mm. What can be seen is that there were a few excellent guides with very little mode conversion. There were also quite a few very poor waveguides with 13% depolarization for TM modes and 32% depolarization for TE modes. Finally, there were a number of waveguides between two extremes. On the whole, however, the TM modes have roughly 2.5 times less mode conversion than TE modes.

Clearly fabrication techniques must avoid irregular sidewalls if depolarization is to be eliminated.

C. Depolarization in Directional Couplers

Table III-2 shows the depolarization in directional couplers for two different devices. These correspond to the two different directional couplers used in the ring interferometer. The nomenclature is the same as in section I. It can be seen that there is a strong tendency of the coupled power to be converted from the input polarization.

In order to analyze the polarization characteristics of the output of a directional coupler, we plot the power out the two arms as a function of the angle of the analyzer. This data is shown in Figure III-8. The value of the signal with the analyzer rotated to 90° represents the amount of depolarization in each of the arms, since the input polarization was TM, defined as angle 0°. It can be seen that the light out each arm is partially polarized, but the degree of polarization of the coupled light is very small.

D. Depolarization in Ring Interferometer

Finally we measured the polarization of the output of the interferometer #4, shown if Fig. III-9. This particular device had a polarization of approximately 50%. It can be seen that the angle of maxium polarization is not perpendicular to the plane of the waveguide. The maximum measured at angle 20° represents a real, experimentally measured angle. This polarization rotation was often observed and differed from sample to sample.

Table III-2. Measurements of Depolarization in Directional Couplers

TM Input	Input Channel TM	Input Channel TE	Cross Channel TM	Cross Channel TE	Total Power Out	Total Coupling Efficiency
D.C. #1						
Power (ARB. units)	80	50	10	30	170	
% of Total	47	29	6	18		24%
% depolarization	38%		75%			
D.C. #2						
Power (ARB. units)	100	62	22	4	188	
% of Total	53	33	11	2		13
% depolarization	38%		15%			
D.C. #3						
Power (ARB. units)	140	38	26	16	220	
% of Total	64	17	12	7		19%
% depolarization	21%		38%			
TE Input - D.C. #1						
Power (ARB. units)	20	20	10	0	50	
% of Total	40	40	100	0		20
% depolarization	50%		100%			

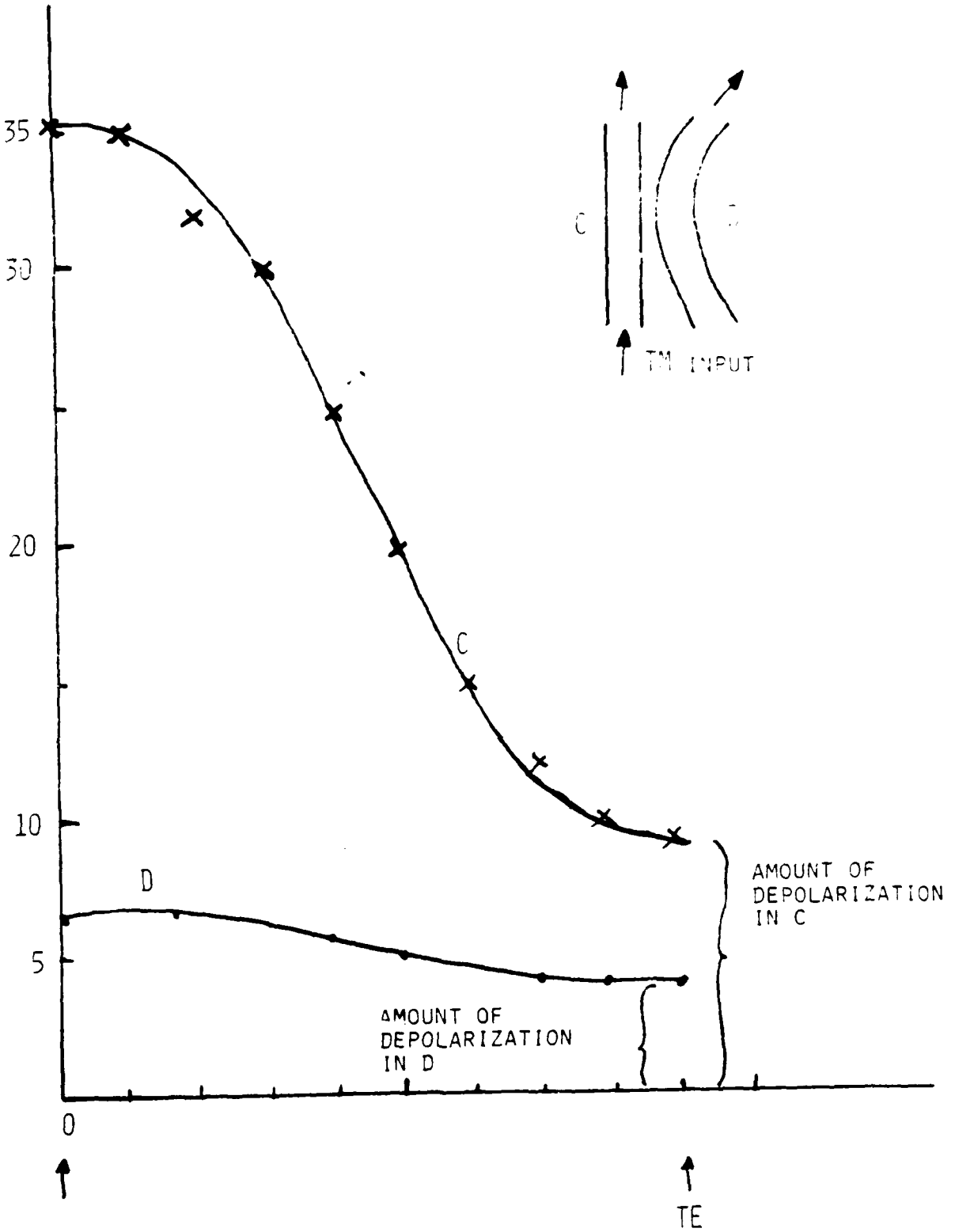

Fig. III-8 Depolarization in a directional coupler

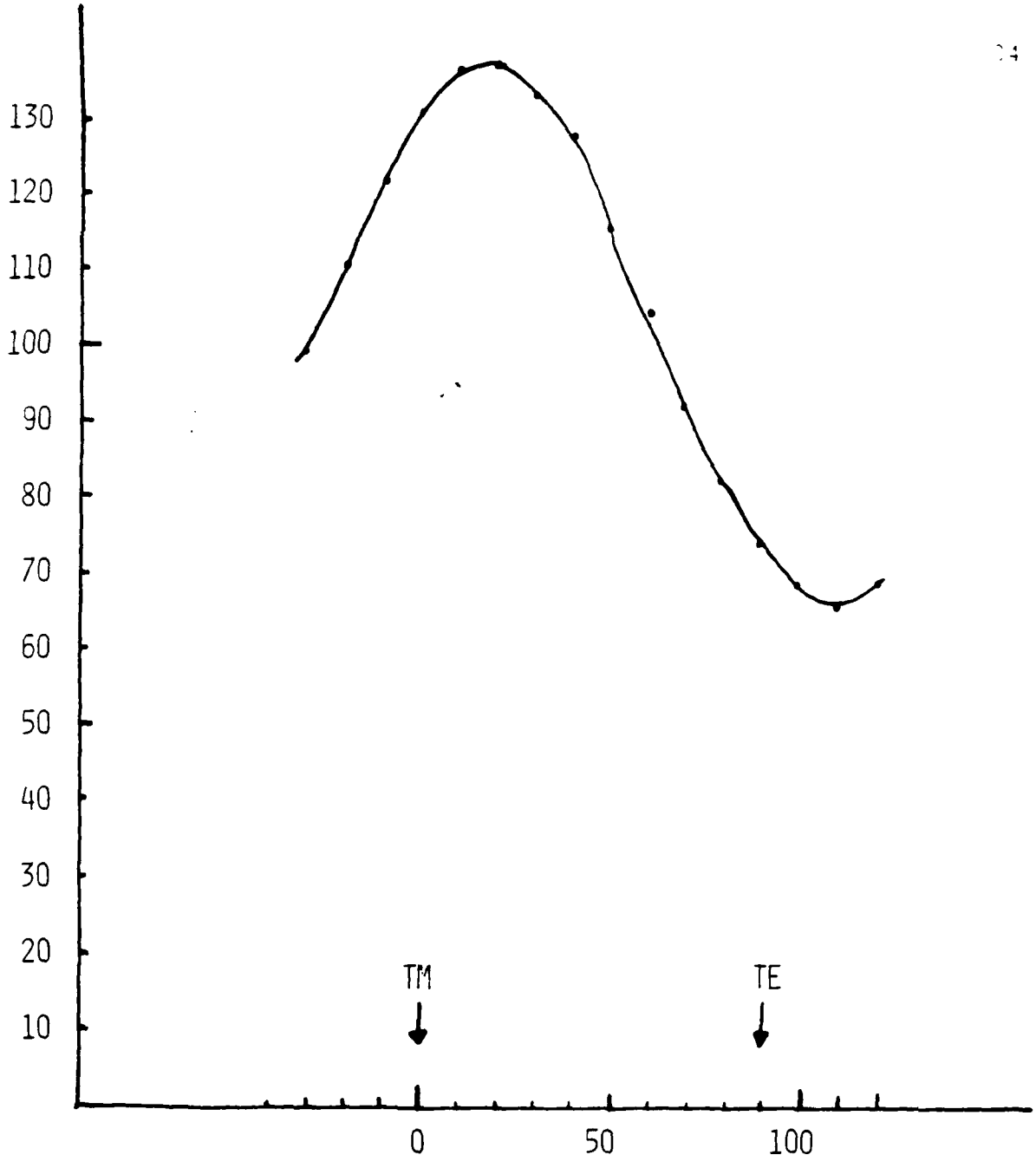

Figure III-9. Output of interferometer as a function of angle of analyzer

The degree of polarization depended on alignment. Using TM input, the percent of the output in the TE polarization was measured for various alignments. With the device optimized for maximum output, 2% depolarization was measured. With the device set for the lowest order mode in the straight-through channel, the depolarization in the output channel was 30%. Finally, with the alignment set so that the straight-through channel had a high order mode, the depolarization on the output channel was 31%. It thus appears that operating the ring in a low order mode causes more depolarization.

We made attempts to reduce the depolarization by annealing the waveguides. We heated the samples at 400°C for 15, 30, 60 and 90 minutes. In each case the depolarization remained. Further annealing destroyed the waveguiding. These results do not agree with reported results in BK7 glass (Iguchi, SPIE, May 1983).

E. Theoretical Analysis of Depolarization

We have not been able to complete a study of the theory of depolarization due to edge roughness of channel waveguides. However, we believe that this effect has a reasonable explanation, based on its similarity to depolarization in cylindrical waveguides due to elliptical nonuniformities.

It is well known that edge roughness will cause mode-conversion. Marcuse has given a theoretical calculation for this effect in planar guides. Under this assumption, no polarization conversion occurs. He has also given a calculation for polarization conversion in circular waveguides due to elliptical imperfections. The case we have here is somewhat between the two cases. In rectangular waveguides, there is no separation between the two polarizations, but they will be coupled by imperfections. We can estimate this by calculating the dispersion curve for the rectangular waveguide using the effective index method. We will then know the period of perturbations which will lead to mode conversion. The depolarization comes from the rectangular nature of the waveguide. Calculations are required to prove that polarization conversion results from edge roughness, and to verify the experimental results.

IV. DIRECTIONAL COUPLERS

Before we fabricated the ring interferometer, we did measurements on directional couplers, in order to determine the required spacing to couple onto and off of the ring waveguide.

The geometry of the directional coupler mask is shown in Figure IV-1. We made a series of devices using this mask, with different ion exchange times. The measured coupling coefficient as a function of ion exchange time is also shown in Figure IV-1.

Prism coupling was used to excite the straight channel guide. The coupling efficiency determined by measuring the output power in both the straight and curved guides is given by

$$\eta = [P_C / (P_C + P_S)] \times 100.$$

The initial increase and then decrease in coupling efficiency reflects the effects of lateral diffusion which alters both the waveguide width and the distance of closest approach for the waveguides.

The lack of coupling for short diffusion times indicates that the waveguides were separated too far apart for coupling to take place. As the diffusion time is increased, diffusion proceeds under the mask; the effective guide width increases and the guide separation decreases. From data to be presented in Section V for the guide thickness as a function of diffusion time, we have plotted values for guide thickness under those for the ion exchange time. Consider Fig. IV-2a. It can be seen that the guide separation decreases by approximately twice the waveguide thickness. It is then possible to plot the coupling efficiency as a function of waveguide separation, shown in Fig. IV-2b. The data show that the waveguide separation for maximum transmission is approximately 5 μm. For too long a diffusion time the waveguides merge and the coupling efficiency is ~10%.

The theory for the coupling efficiency of variable spacing directional couplers has been published by Finlayly. Using a similar computer calculation, we obtain the coupling efficiency as a function of guide spacing given by Fig.IV-3. This model is very approximate. However, for our geometry, the theory shows the salient features. If the waveguide separation is too large, no

Fig. IV-1. Fraction of directional coupling as a function of ion exchange time.

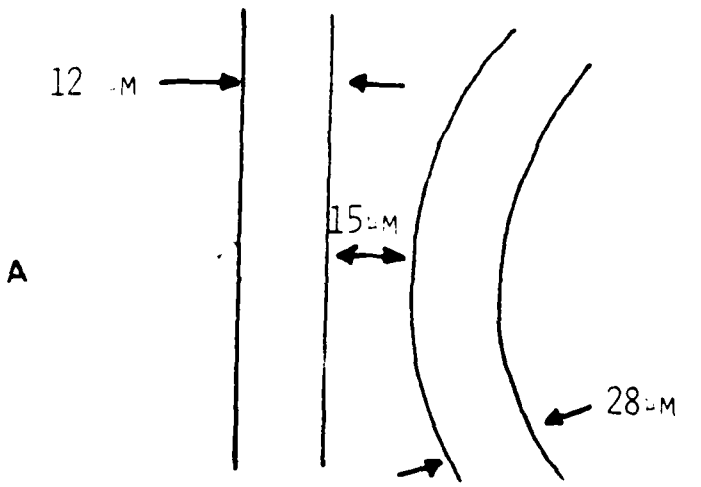

A) geometry of directional coupler mask

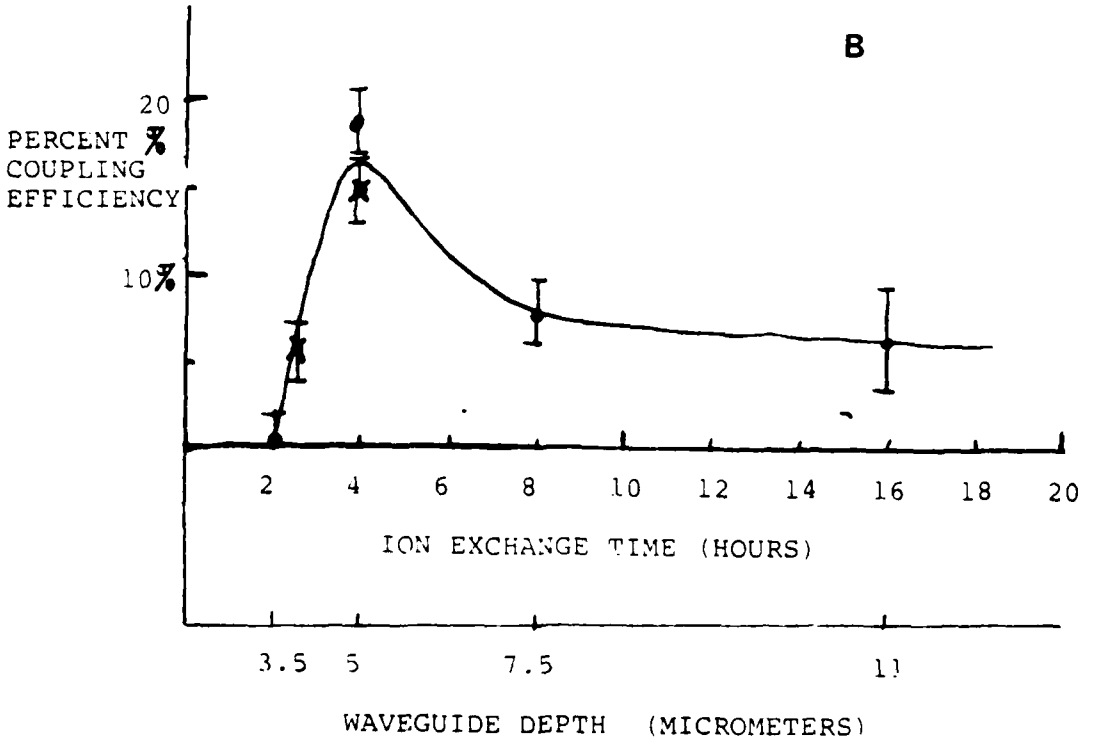

B) percent coupling efficiency

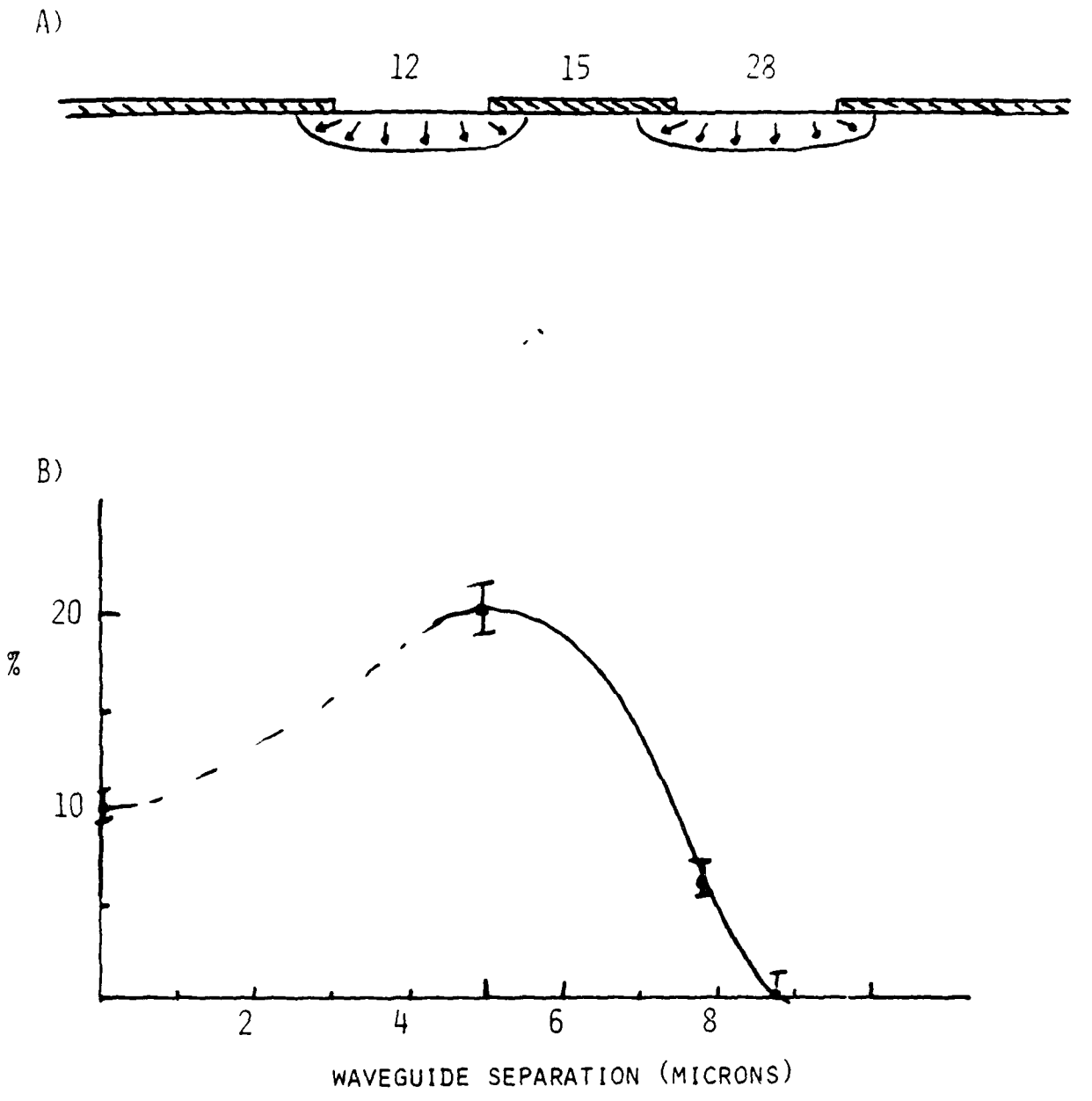

Fig. IV-2. Undercutting of mask with ion exchange. A) geometry of effect; B) percent coupling as a function of assumed waveguide separation.

Fig. IV-3. Theoretical coupling efficiency for a directional coupler with waveguide width w as a function of waveguide separation. Solid and dotted lines are for the lowest order mode. Dashed line is an estimate for the m= 6 mode.

coupling occurs. There is in fact a particular separation for optimum directional coupling. The actual numbers are not in agreement with the experimental measurements, however. That is, large coupling coefficients are predicted only for smaller waveguide separations. The reason for this was discovered by looking at the mode profiles of the light coupled across from the straight to the curved channel waveguide. We find that only higher order modes are coupled with high efficiency.

The calculation of Fig. IV-3 was for lowest order modes only. To achieve good agreement with theory and experiment, therefore, we must perform the calculations for the higher order modes. While not doing a numerical analysis, we may estimate the mode-dependence of the coupling efficiency using some simple arguments. The coupling efficiency is given by

$$\eta \propto e^{-qd}$$

where d is the separation between the waveguides and q is the exponential fall-off of the light outside the waveguide. The other mode-dependent factors in the coupling efficiency are not so strongly varying, when the waveguides are separated rather far apart.

The approximate mode-dependence of q is given by

$$q^2 = \beta^2 - n_s^2 = (\beta - n_s)\ (\beta + n_s) \simeq 2\, b\, n_s (n_f - n_s)$$

where b is a parameter defined and plotted by Kogelnik. From the plot of b, it can be seen that approximately

$$b_m \sim b_o \left(\frac{M-m}{M}\right)$$

or

$$q_m \propto \sqrt{\frac{M-m}{M}} \quad .$$

Thus, the value of q for the highest order mode in terms of the lowest order modes is $q_M = q_o/M^{\frac{1}{2}}$. Since

$$\frac{\ell n\ K_m}{\ell n\ K_o} = \frac{q_m}{q_o}$$

then

$$K_M = K_o^{1/\sqrt{M}} .$$

In the waveguides we studies, M=6 so $K_6 = K_o^{0.41}$. Using this expression, we plotted K_6 as a dotted line on Fig. IV-3. This shows that a coupling coefficient of 20% for a separation of 5 μm is a reasonable result.

When the waveguides were excited by endfire coupling, which tends to excite lower order modes, the directional coupling efficiency in all cases was found to be less than with prism input coupling. In fact, using the endfire method of excitation, it was found that the directional coupling efficiency was very sensitive to lateral alignment.

The importance of the modes of the guide on the coupling coefficient was confirmed when photographs were made of the farfield pattern of the output arm of the directional coupler when used in the ring interferometer. This was shown in Fig. II-6. The fact that this was the highest order mode of the guide is clearly in evidence.

V. WAVEGUIDE FABRICATION TECHNIQUES

We developed two techniques for fabrication of waveguides in glass substrates. The last year we used ion exchange from KNO_3 melts. This technique will be described first. Previously, we used diffusion from metallic silver films. Although very low loss waveguides were obtained with this technique, the refractive index change was too low unless the diffusion took place in the presence of an electric field. We found that the electrode tended to introduce loss and were not able to satisfactorily eliminate this problem. We therefore abandoned this effort. Diffused waveguides are described in section B.

V.A. Fabrication of Waveguides by Ion Exchange from KNO_3 Melts

V.A.1. Introduction

The fabrication technique for ion exchange involved immersing the substrate in a KNO_3 melt for several hours. Typical temperatures and times are 400°C for 2 hours. The conditions to obtain a single mode depend on the sodium composition of the substrate glass. Initial measurements were made in microscopic slides. Finally, the ring resonator was fabricated in Kodak lustra glass plates. We were not able to obtain single mode waveguides in this glass when the ion exchange was performed at 400°C. Lowering the ion exchange temperature to 350°C should make it wasier to obtain single mode waveguides.

Waveguides fabricated by ion exchange from KNO_3 melts at 400°C typically have a $\Delta n \simeq 6 \times 10^{-3}$. Figure V.1 shows the index profile of two such planar waveguides. The WKB method was used for determining the refractive index profile. For this index change, radiation losses in 2 cm radius of curvature channels are negligible. A few words of caution in the fabrication of waveguides from KNO_3 melts:

1. Use a metallic crucible, preferably aluminum. Because of the difference in thermal expansion between glass and KNO_3, glass petri dishes crack when allowed to cool while containing KNO_3. This difference in thermal expansion coefficients also causes stresses in the glass samples. The glass samples must

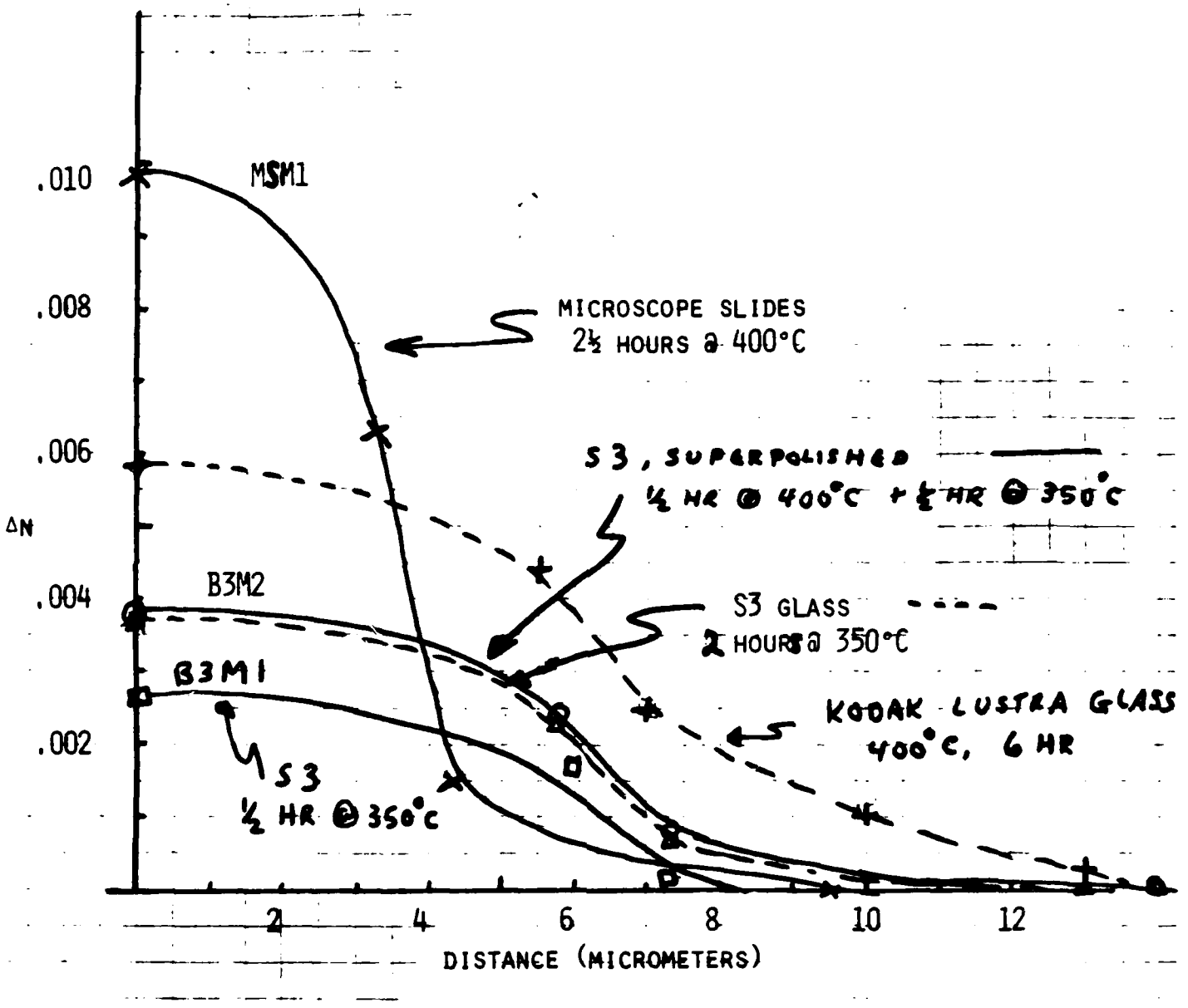

Fig. V-1. Refractive index profile for waveguides fabricated by ion exchange from a KNO_3 melt, determined by WKB method.

therefore be removed from the hot melt after the designated ion exchange time and be allowed to cool outside the melt to avoid cracking.

2. For channel waveguides, once the samples have been removed from the melt and are cool, the residual KNO_3 should be immediately washed away from the sample with water if the waveguiding channel is to remain delineated by the aluminum film. We have found that the KNO_3 crystallized on the glass substrate dissolves aluminum.

V.A.2. Measurement of Waveguide Characteristics

A log-log plot of the effective waveguide depth versus ion exchange time is shown in Fig. V.2. From the slope and intercept of the graph we obtain an expression for the effective depth as a function of the ion exchange time in hours. Because the composition of microscope slides varies from batch to batch the expression for the time dependence of the effective waveguide depth given here serves only as a guidline for waveguides fabricated in these substrates by ion exchange from KNO_3 melts. Here we see that a two-mode guide with $Z_{eff} \simeq 3$ μm is fabricated for ion exchange time of 1½ hrs. Single mode guides are fabricated for ion exchange times of 1 hour.

V.A.3. Fabrication of Channel Waveguides in Glass

The channel is defined by an aluminum mask. The primary step in fabrication of high quality waveguides in glass substrates is the proper cleaning of the substrate for deposition of the metallic film. This step is crucial since good adherence of the evaporated metal film to the substrate minimizes breaks in the metal films during subsequent processing and as such reduces one potential source of loss. All processing must be done in a clean room to avoid dust contamination.

We have found the following glass cleaning technique to work quite well and have obtained good adherence with Ag and Al films up to 3000 Å thick. This should be done in the clean room.

A. Glass Cleaning Procedure

1. Scrub samples with cotton swabs in tap water and detergent mix (Alconox).

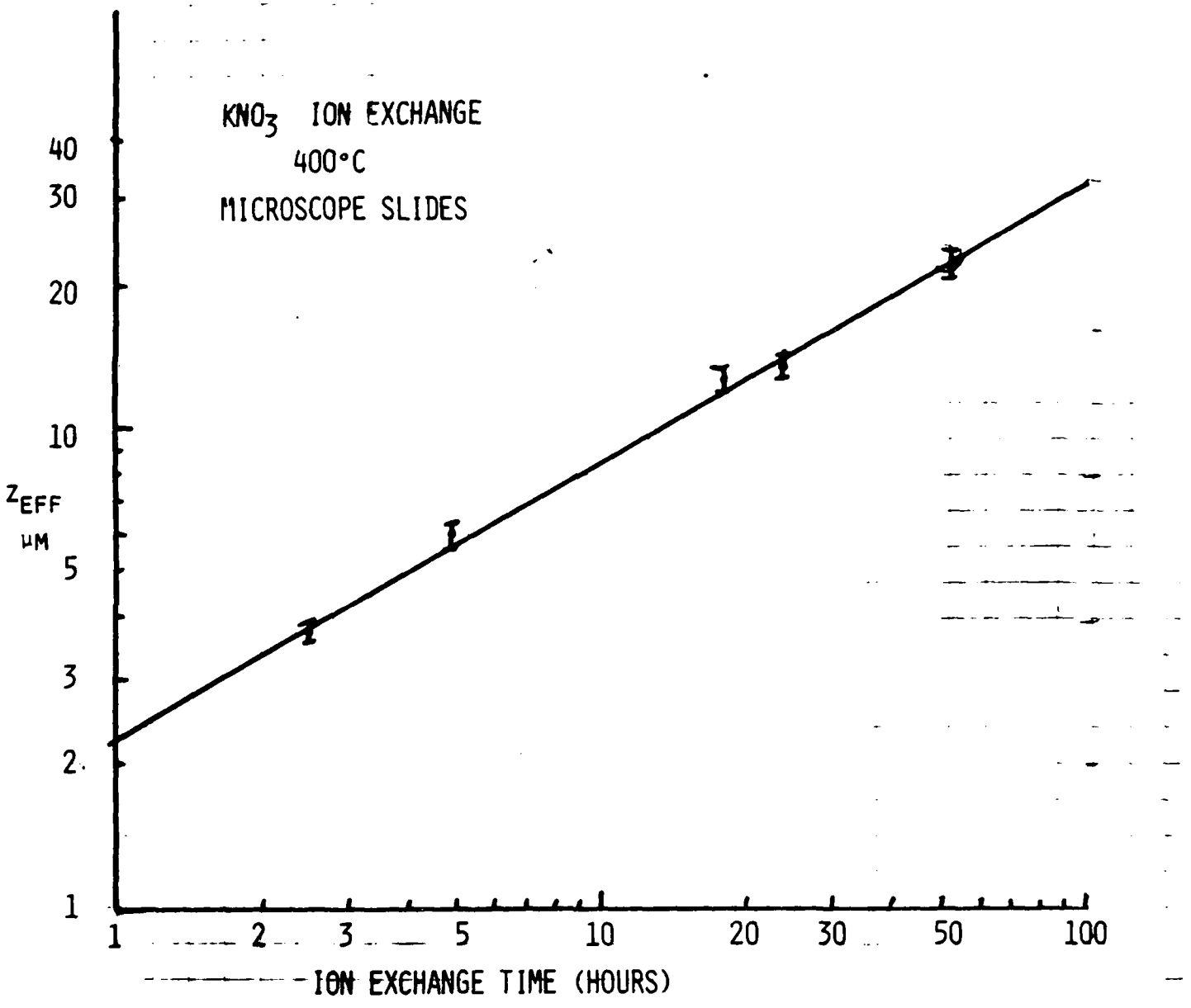

Fig. V-2. Waveguide depth as a function ion exchange time; planar guides. z_{eff} is the depth for the 1/e of the refractive index increase.

2. Rinse with tap water
3. Rinse with DI water
4. Scrub with cotton swabs while in boiling Acetone
5. Scrub in boiling TCE
6. Rinse in Acetone with ultrasonic
7. Scrub with mixture of boiling DI water, Orion and NH_4OH
8. Wash thoroughly DI water
9. Force dry in Nitrogen
10. Bake in oven at 250 - 300°C for two hours and immediately deposit metal.

B. Metal Film Deposition

Fabrication of channel waveguides by ion exchange requires the deposition of a metal film to bar ion migration from regions about the channel. Metal films of Titanium and gold chrome have been attempted to act as such a barrier against K^+ ion migration from KNO_3 melts. Gold chrome was found to dissolve in the KNO_3 melt and as such is unsuitable. Titanium metal films were found to adhere very well to the glass substrate and channel definition prior to ion exchange was achieved by using a dilute HF etch. However, removal of the Titanium mask from the substrate after ion exchange was found to be very difficult. In fact the surface of the substrates from which the titanium was successfully removed were found to be attacked by the HF solution. So we switched to Aluminum as a mask to bar ion exchange from regions about the channel because it is readily etched by both acids or hydroxides even after ion exchange. However, because positive photoresist developers contain hydroxide, the deposited aluminum film must be no less than 3000 Å thick. With films of this thickness one avoids pitting of the film during photoresist processing. Etching of the aluminum to delineate the channels is accomplished by using an acidic etch which does not attack the protective photoresist coating.

Deposition of the Al metal film is done at pressures of $\simeq 10^{-6}$ torr. To enhance adhesion and to obtain a good metallic

film, Aluminum is slowly melted in the crucible and rapidly evaporated. Typically 18 inches of 62 mil Aluminum wire evaporated on samples positioned 12 inches from the source yield 3000 Å thick Aluminum film. Aluminum film thickness can also be monitored during deposition by using the crystal thickness monitor on a material number setting of 370.

C. Photoresist Processing

Several positive photoresists have been used to define channels in the aluminum film. We have found that Shipley 1370J photoresist spun on at 5000 r.p.m. for 30 secs gives a 1 μm thick coating which gives negligible undercutting during the etching process.

After spinning the photoresist is prebaked at 90°C for ~20 minutes before exposure. Patterns from a mask are transferred to the photoresist coated substrate with the aid of a mask aligner. Exposure times range from 4 secs to 10 secs depending on the intensity (age) of the high vacuum mercury lamp. After exposure the patterns are developed using Shipley Microposit 351 photoresist developer diluted with D.I. water in a ratio of 1:5 and then post baked at 90°C for 30 minutes. Post-baking has been found to enhance the adhesion of the photoresist to the metallic film and as such minimize undercutting during etching.

D. Etching

An acid etch is used to define the channels in the Aluminum film. This consists of:

Nitric acid - 3%
Phosphoric acid - 77%
Acetic acid - 4%
D.I. water - 16%

The etch does not degrade in time but it is best not to reuse it.

Best results are obtained when the etch is heated to 55°C (temperature control is critical) and when the sample is removed as soon as the first bubbles started forming on the aluminum. The substrate is then rinsed in DI water and the protective

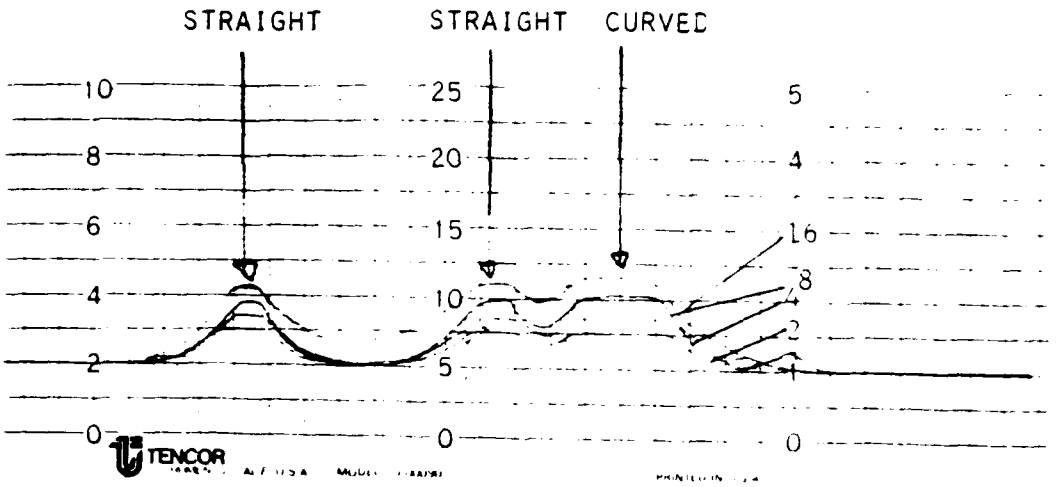

Fig. V-3a. Profilometer traces of waveguides fabricated by K^+ ion exchange for 2,4,8 and 16 hrs.

Figure V-3b. Microscope pictures of waveguide channels after ion exchange.

photoresist coating removed with acetone or photoresist stripper.

E. Ion Exchange in Channel Waveguides

The substrates are then placed in a container with KNO_3 and heated to 400°C for the required period of time. At room temperature KNO_3 is polycrystalline, but above 350°C, it melts and flows around the glass substrate, providing the melt for ion exchange. Since the substrate and sample are heated together, there is approximately a 20 minute heating time added to the measured ion exchange time. The reason for heating the sample and the KNO_3 together is to avoid any undue thermal stress.

It was observed that after ion exchange and with the Aluminium film etched away from the substrate, some of the channel waveguides were still visible. Profilometer measurements (Fig. V-3a) showed that there was an elevation formed in the glass at the position of the waveguide. Fig. V-3b shows a low contrast picture of this effect. This height change was found to vary monotonically with ion exchange times (Fig. V-4a) for times extending up to 16 hours at which point the ridge was approximately 0.3 μm high. Associated with this height change is a widening of the waveguide channel. For channels defined by aluminium masks 10 μm - 30 μm wide the effective width of the elevation (width at half the height change) varied from 25 μm - 40 μm (Fig. V-4b). The data show that for these channels the guide widens by 15 μm, independent of ion exchange time. The reason for this is not fully understood and may be evidence of undercutting of the aluminium mask.

F. Edge Polishing of Glass

Edge polishing of glass samples is required when endfire coupling into waveguides fabricated in thick glass substrates is desired. This is the last step in the fabrication process and is done after ion exchange.

In edge polishing the sample is placed in a chuck and blocked up with microscope slide blanks. The entire sample and microscope slide assembly are held together with molten black wax. The flat edges of the outermost samples and the sides of all the samples are bevelled with sandpaper or emery board (Fig. V-5) to

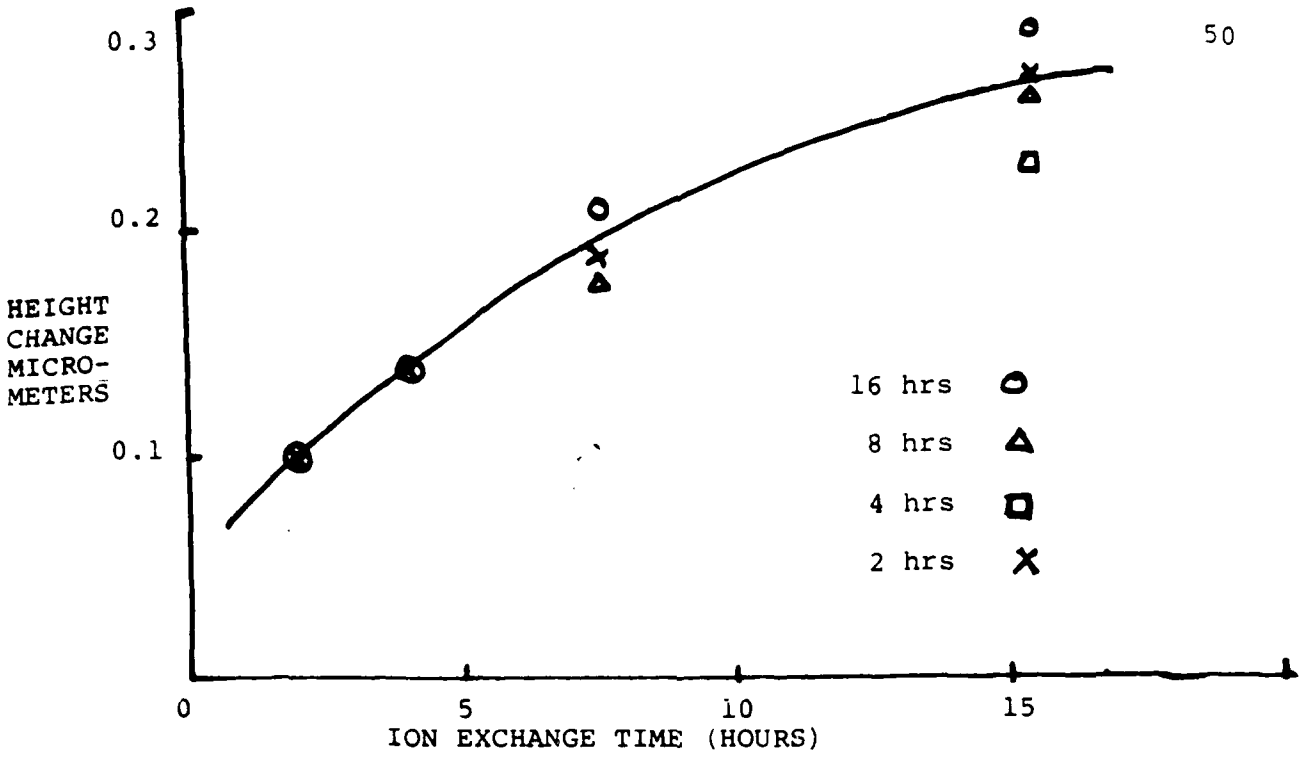

Figure V-4a. Increase in ridge height of channel waveguides as a of ion exchange time

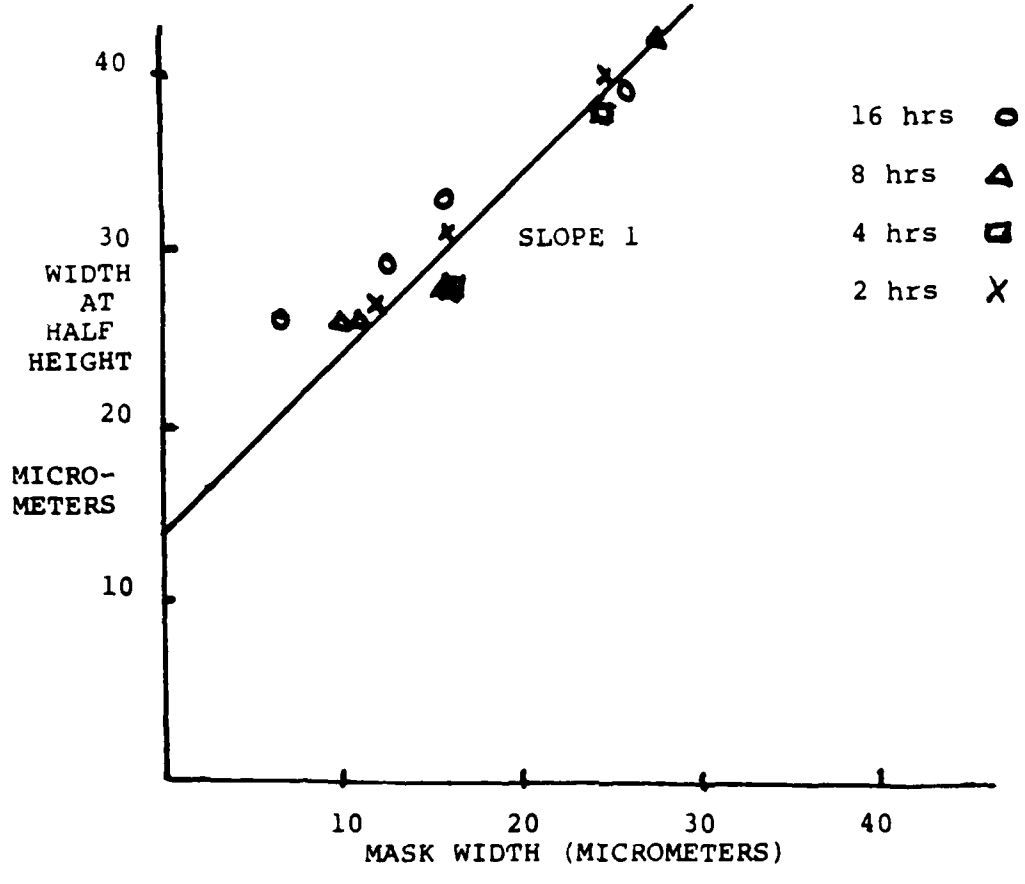

Figure V 4b. Increase in ridge width of channel waveguides

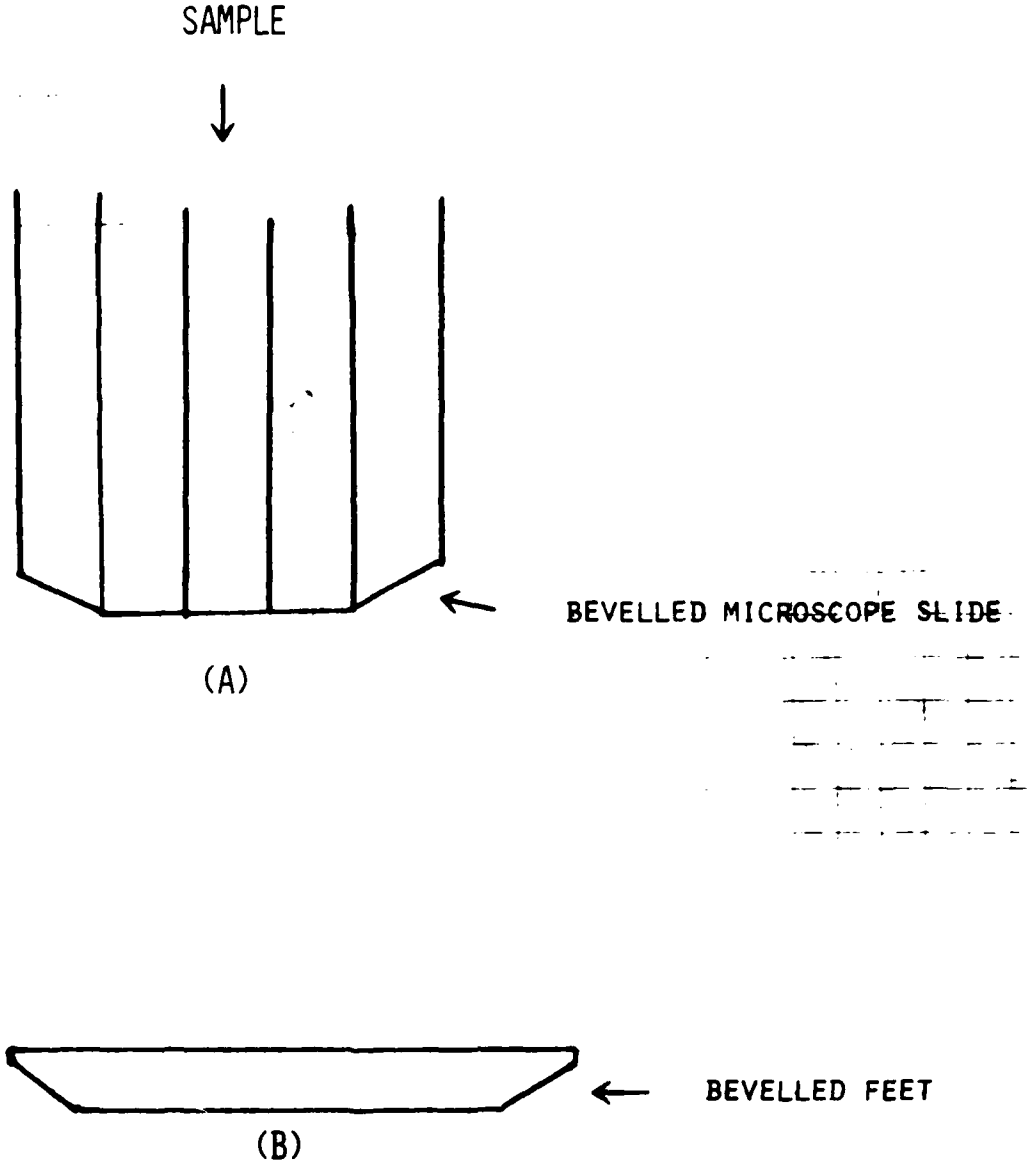

Fig. V-5. A) For edge polishing of glass the outermost microscope slides are bevelled to avoid chipping. B) The feet attached to the lap are made from end - bevelled microscope slides.

minimize surface scratching caused by broken chips of glass. Glass feet are also attached to the base of the chuck with black wax; all sharp glass edges bevelled. After the sample and feet are attached to the chuck, the assembly is allowed to cool and while still warm to the touch it is transferred to an optical flat for final cooling. This is to ensure that the sample and blocking slides are level with the feet.

Initial grinding of the sample is done using 22.5 μm aluminium oxide powder on a grooved lap. This coarse grit accelerates the grinding process and is continued until the surfaces are seen to be evenly ground. The chuck and lap are then thoroughly rinsed with tap water and scrubbed to remove any residual coarse grit. This procedure is repeated using 600 aluminium oxide grit and then 3.0 μm grit. After the sample is properly ground the chuck is washed thoroughly in warm soapy water before polishing.

A 3/4 inch pitch polishing lap is prepared using 50% soft optical pitch. The pitch is melted and poured onto a flat metal lap. To contain the molten pitch on the lap masking tape is wrapped around the edge. When the pitch is firm, the lap is turned over on an optically flat surface and allowed to cool.

After cooling, grooves are cut into the pitch surface; these act as traps for the coarser polishing particles which are washed away during polishing. Initial polishing is done using 1 μm aluminium oxide powder. This grit is used until the feet and sample surfaces appear well polished. The polishing lap and chuck are then rinsed and scrubbed and further polishing is continued using .05 μm aluminium oxide powder. An alternative to using 1 μm and .05 μm polishing powders is to use Syton.

B. Optical Waveguide Formation by Solid-State Diffusion From Silver Films

1. Without Electric Field

A thin film of silver (2000Å) is vacuum deposited on a glass substrate. Proper deposition of the silver film on glass requires pressures of the order 10^{-6} torr. The deposition is done much more slowly than aluminium deposition. The adhesion of the silver film to the substrate is generally not as good and as such any required

processing should be done as soon as possible. Typically 10 inches of silver give a 3000 Å thick film on a substrate positioned at 12 inches from the source.

After deposition, ion exchange of the silver with the sodium in the glass occurs by heating the sample to temperatures between 300°C and 500°C. Diffusion times range from 10 minutes to three hours, resulting in guides with thicknesses from 10 μm to 100 μm. The change in refractive index in microscope slides is approximately 10^{-3}.

Photo-resist processing is used to provide the optical circuit in the silver film before diffusion. We have been most successful with negative photoresists.

2. With Electric Field

In order to obtain a higher refractive index, we applied an electric field during diffusion. This was done by overcoating both sides of the sample with electrodes and applying a voltage between the two faces of the substrate. Fig. V-6 shows two mode profiles for identical conditions, except for a change in temperature. Clearly for B3E1 there was depletion of the silver film at the surface, since the higher temperature caused a reduced refractive index at the surface.

For identical conditions except for a variation in voltage, we obtain Fig. V-7. Thus voltage causes $\Delta n \propto V$, but the thickness is determined by the time and temperature.

When the temperature is decreased so that the depletion of the silver film does not occur, then the index increase at the surface is roughly proportional to applied field, as shown in Fig. V-8. Similar data was obtained in S-8000, except that waveguides are fabricated at lower temperatures and comparable fields results in smaller values of Δn.

Along with electro-diffusion of waveguides, in channel waveguides there appeared a depression in the surface of the substrate, as shown in Fig. V-9. This made it impossible to prism-couple into electro-diffused waveguides. This is one reason why electro-diffusion was not pursued further. The other reason was an increase in loss, described in Section VI.

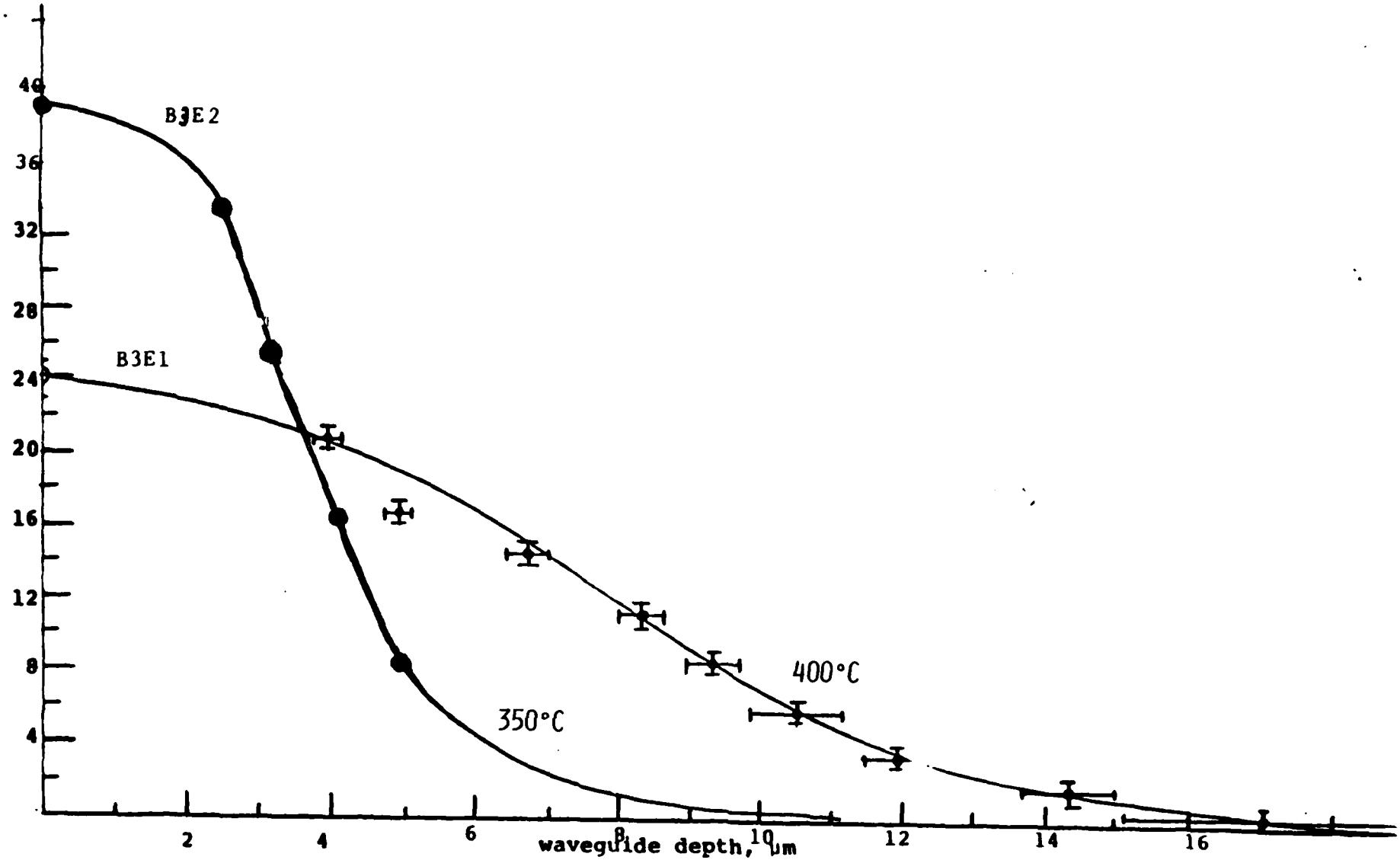

Fig. V-6. WKB refractive index profile for waveguide fabricated in S3 glass by field assisted diffusion with an electric field of 40 V/mm applied for 15 min.

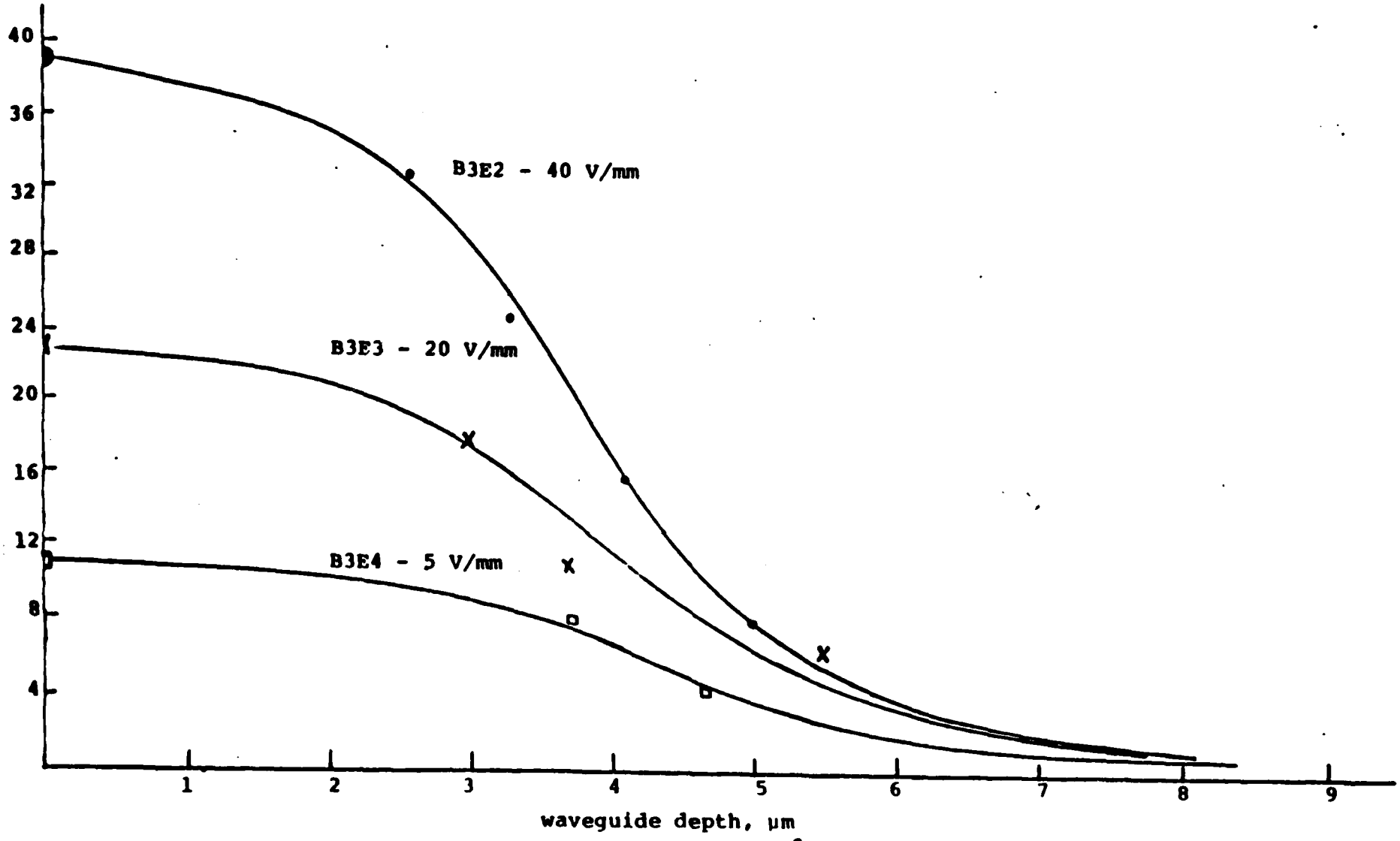

Fig. V-7. Index profile for guides fabricated at 350° C with electric field applied for 15 min.

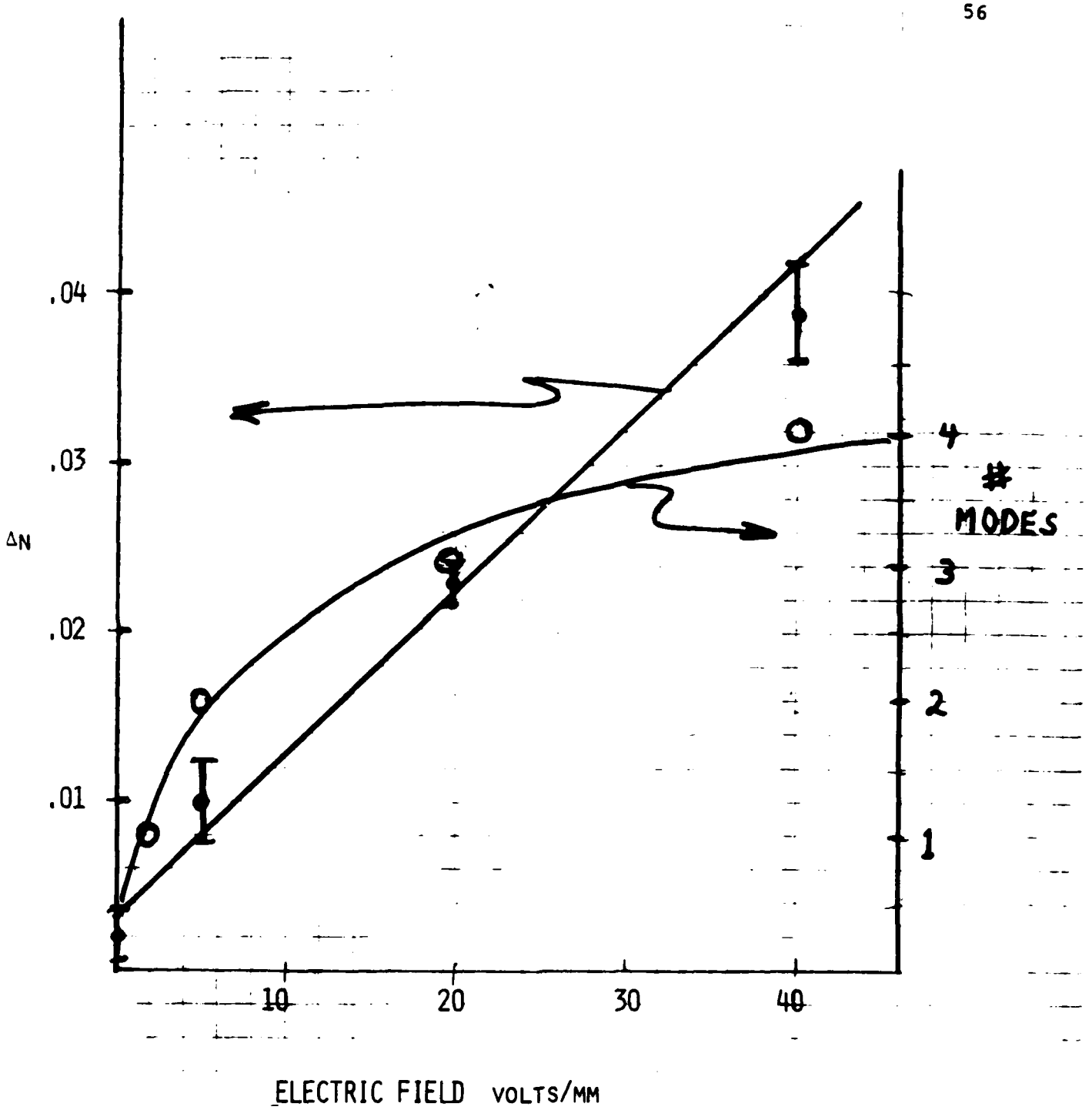

Figure V-8. Dependence of Δn at the surface on applied field during diffusion of 2000Å film into S-3 glass at 350° for 15 minutes. Also, number of modes in a guide as a function of applied electric field.

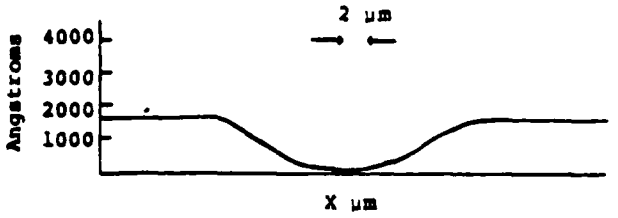

Figure V-9a. Typical profilometer trace of groove formed when electro-diffusion is done at elevated temperatures. X is position measured along glass surface.

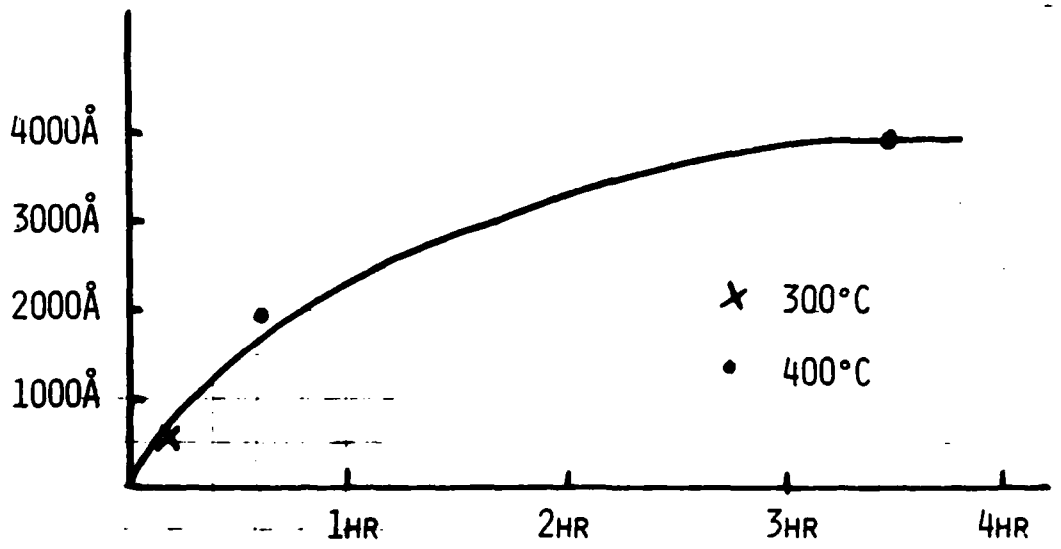

Fig. V-9b. groove depth vs. diffusion time

VI. LOSSES IN GLASS WAVEGUIDES

A. Planar Waveguides

In the early months of this contract we made a study of the losses in waveguides using different glass substrates. The purpose of this study was to determine those factors which contribute to loss in glass waveguides and to estimate the performance expected in ring interferometers.

In this study we proved conclusively that fining agents added to optical glass to eliminate air bubbles cause reduction of those ions introduced to form the waveguide. This has been shown by comparing losses in waveguides fabricated by the same technique in different glass substrates.

Figure VI-1 shows the losses measured in a number of planar waveguides fabricated on different substrates. The technique used was diffusion of silver ions. Samples K1 and V1 represent two different brands of microscope slides. A large variation was seen from box to box within a brand as well as from brand to brand. The samples S-3 and S-8000 represent two compositions of Schott glass, especially fabricated without fining agents. The former is soda-lime silica glass and the latter is phosphate glass.

In previous work we demonstrated that a loss which decreases with mode number is due to scattering or absorption within the volume of the waveguide, while losses which increase with mode number are due to the surface of the waveguide [Findakly and Garmire, Appl. Phys. Lett. 37, 855 (1980)]. Thus the S-3 glass has a loss which depends on the silver diffusant, but S-8000 glass has a loss due primarily to surface roughness. With such high loss in the S-3 glass, we determined that not all reducing agents were removed from the glass. Indeed, the glass included arsenic and titanium. We therefore obtained S-3 glass prepared without titanium or arsenic, and obtained waveguides with much lower loss (labelled S3*). It is with this glass that low-loss resonators should be obtainable.

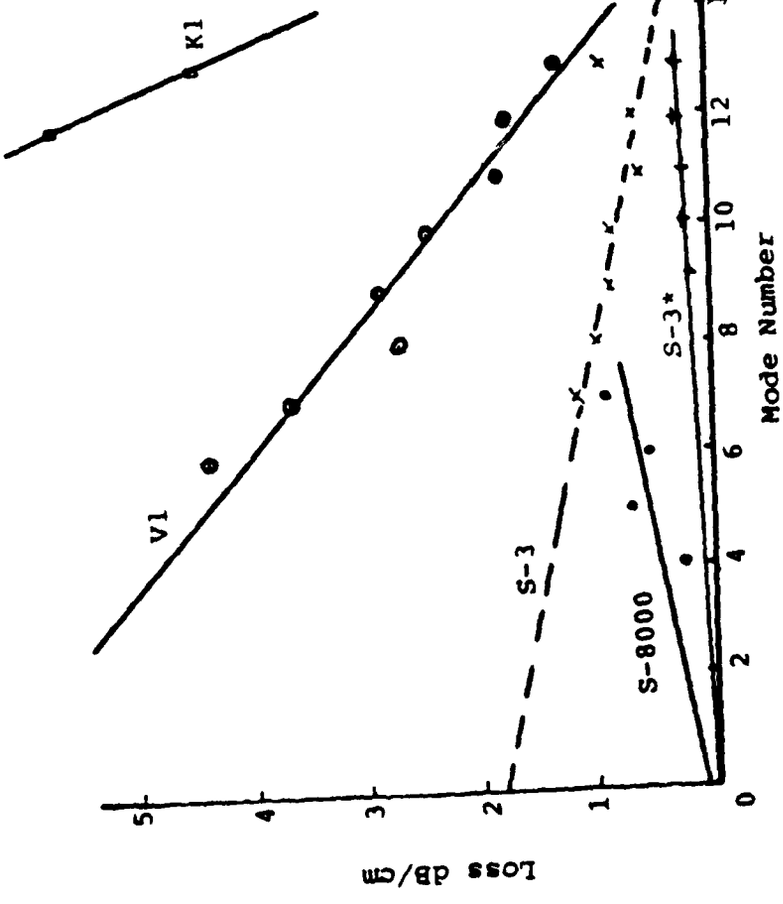

Fig. VI-1 Mode-dependent losses for microscope slides V1 and K1 and optical glasses, S-8000 and S-3. S-3* represents S-3 glass without arsenic or titanium.Waveguides were fabricated by diffusion of silver film.

The very low loss in S3* was measured using the three-prism technique. For mode numbers smaller than 9, the coupling efficiency was too small for the signal to be above the noise limit of the detector, and to measure meaningful loss. Measurements could not be made for these modes. However, the average loss in S3 glass was ~0.14 dB/cm.

Since these highly multimode guides were not suitable for the ring resonator, we studied field-assisted (eletro-thermal) diffusion and measured its losses. These waveguides had much higher values of refractive index and were not so deep. Typical losses are shown in Fig. VI-2. We discovered that the gold anode was contributing loss to the waveguides, so we used a thick silver film as an anode and observed a much lower loss.

Because of the slope of the mode-dependence of the loss, it can be seen that the loss is primarily due to roughness of the surface. The ten times higher loss which occurs when a field is applied during diffusion is a direct result of the fact that the waveguide is then times thicker. Indeed it was difficult to remove the anode after the field-assisted diffusion. The solution to this dilemma is to bury the guide below the surface. We reported preliminary results on burying the guide which indicate a reduction of a factor of five in loss by burying the guide [Findakly and Garmire, Appl. Phys. Lett. 37, 855 (1980)]. This procedure has not yet been demonstrated on channel waveguides, and remains to be accomplished.

Because of our concern with silver as a diffusant and the electro-thermal process degrading the surface, we decided to study ion exchanged waveguides using melts. Typical losses in planar waveguides are shown in Fig. VI-3. It can be seen that, for waveguides of comparable thickness, the losses are considerably below those due to field-assisted silver diffusion. Again, in these waveguides the higher order modes have greater loss, indicating that for these shallow waveguides the predominant loss mechanism

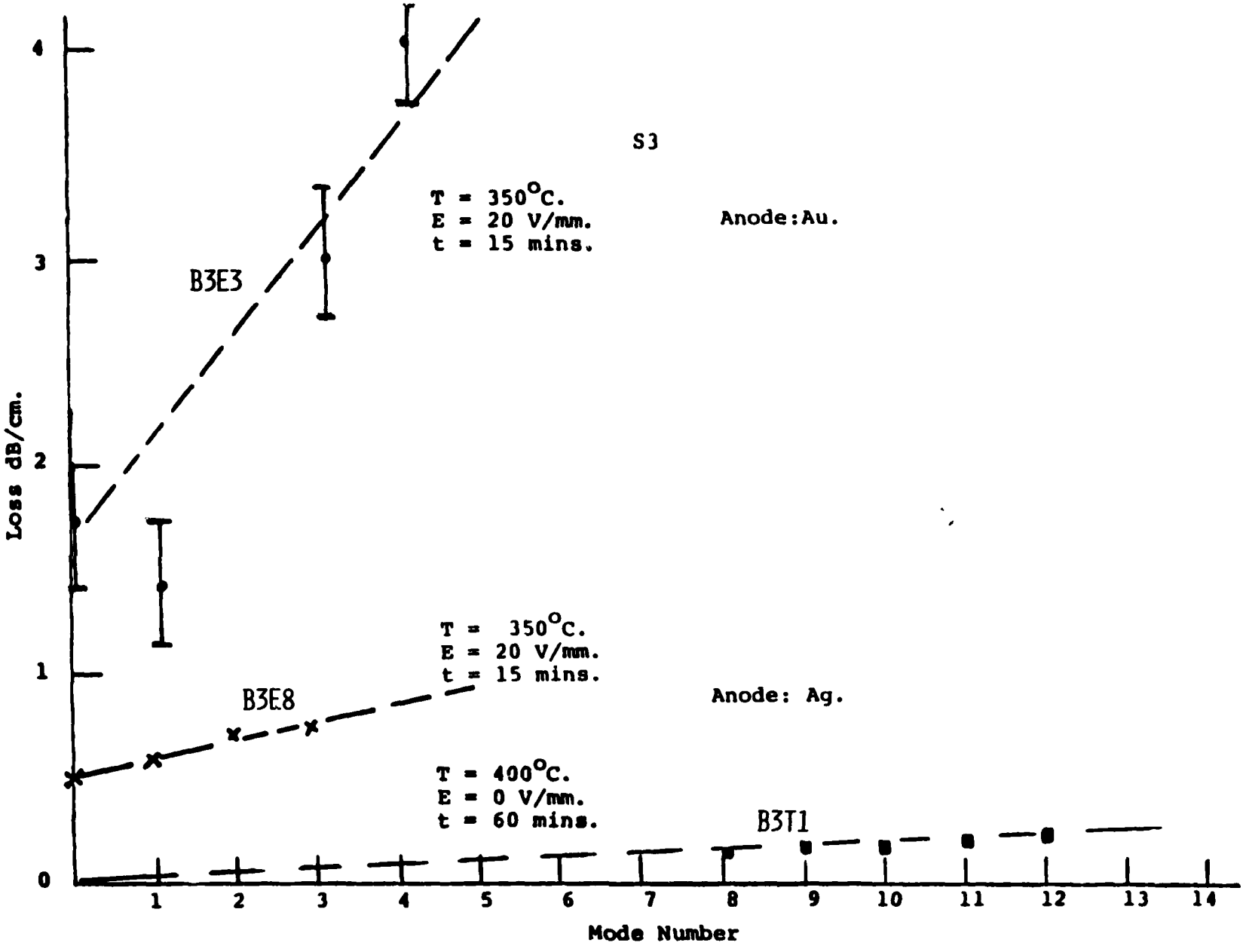

Fig. VI-2 Mode dependence of the losses in waveguides fabricated with and without an applied electric field.

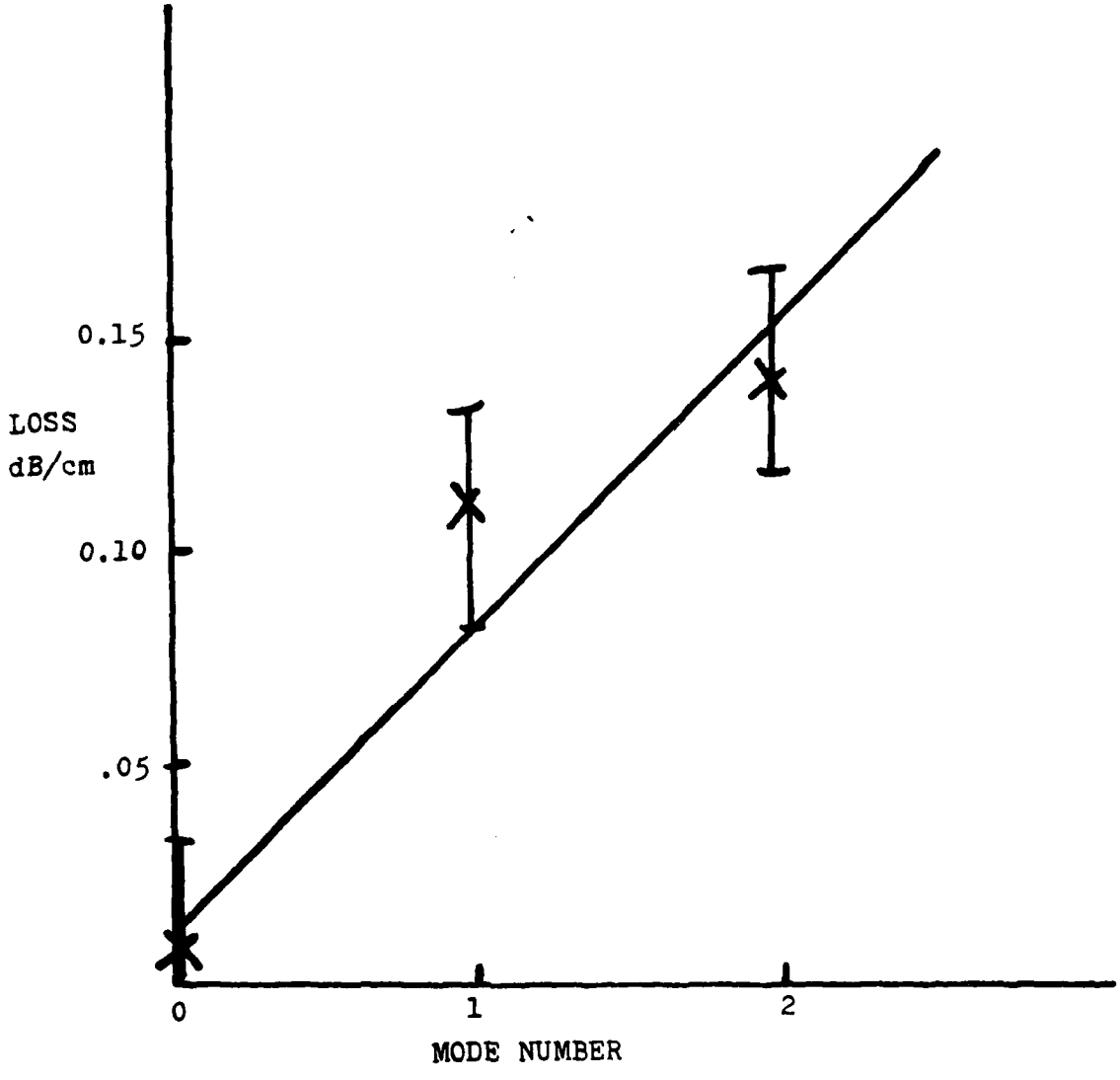

Figure VI-3. Loss of three-mode planar waveguide 6 μm thick fabricated by KNO_3 ion exchange in S3* glass at 350°C for two hours.

is surface roughness. Highly multimode waveguides fabricated in S-3* substrates exhibited such pronounced in-plane and out-of-plane scatter that no definitive measurements of either mode angles or mode dependence of the loss could be made. Because the strong intermodal scatter was observed in the optical glasses and not in microscope slides, we suspect that for these deep waveguides additional scattering losses are caused by subsurface microcracks created during preparation of the glass surface. These suspicions were further strengthened when we observed that there was no change in the intermodal coupling when the substrate was coated with methanol.

B. Channel Waveguides

The losses in curved and straight channel waveguides have been measured using microscope slides as substrates. Typical loss measurements of guides are shown in Fig. VI-4. As is expected because of its 20 μm width, the losses in the straight channel are within the ±0.2 dB/cm error bar of the planar waveguide. The curved channel waveguide was excited by endfire coupling. As such, the 0.97 dB/cm loss measured represents the average loss over all modes. When this is compared to the 0.85 dB/cm average loss in the planar guide, it isseen that for the 3 cm radius of curvature the radiation losses in this waveguide are negligible. This is predicted by theoretical modelling, shown in Table VI-1.

The losses in microscope slides are higher than in S-3* glass and decrease with increasing mode number. This is presumably due to absorption and scatter from fining agents within the microscope slide glass, which are missing in the S-3* glass. The contract ran out before were able to fabricate channel guides in S-3* glass, since we choose the more readily available Kodak Lustra glass for our first ring resonators. However, all data to date indicate losses in the order of 0.1 dB/cm at 0.63 μm in S-3 glass without fining agents.

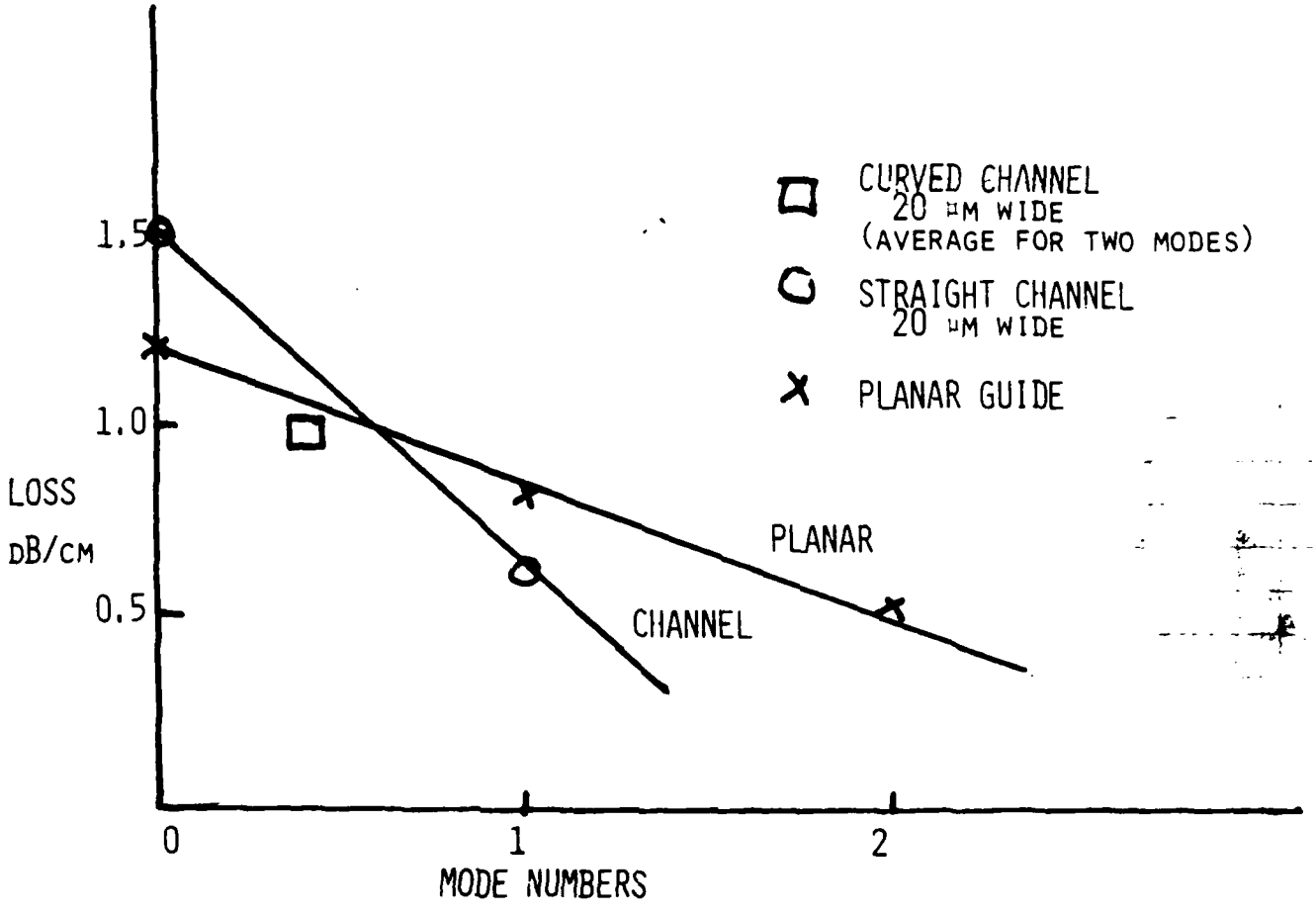

Fig. VI-4 Mode dependence of the loss for planar and channel waveguides in microscope slides fabricated from a KNO_3 melt at 400 C for 2 hours. The loss of the curved waveguide was measured by endfire coupling and is given as a single point on this graph.

TABLE VI -1. Bend Loss in dielectric waveguides

The losses for a bent waveguide are given by Marcatili Bell System Technical Journal vol. 48, 2103 (1969). When the guide is multi-mode, Marcatili equ. 14 gives the loss per radian of bend as approximately

$$R = (n/2\Delta n)^{\frac{1}{2}} \exp(-cR/\lambda)$$

where $c \approx 10\ (\Delta n)^{3/2}$

The following is a table evaluating the loss through 2π radians for various ring radii and refractive index discontinuities

	Loss per revolution in ring				
Δn	R = 0.5cm	R = 1 cm	R = 2 cm	R = 5 cm	5 = 10 cm
.001	100%	67%	7.2%	10^{-7}%	0
.002	9.6%	10^{-4}%	10^{-8}%	0	0
.003	.02%	0	0	0	0
.006	0	0	0	0	0
.008	0	0	0	0	0

Predictions of the ultimate lowest loss expected by our techniques can be made by extrapolating several of our measurements. From the data in Figure VI-3, losses at 0.63 μm the order of 0.1 dB/cm are obtained. Previous measurements on the wavelength-dependence of loss showed that going to 1.1 μm input wavelength reduced the losses a factor of five. At this wavelength, the waveguide previously reported in S3* (Fig. VI-3) would be a single mode. Thus, we expect loss on the order of 0.02 dB/cm.

Further reduction in loss can be achieved by burying the guide below the surface. We demonstrated a reduction of loss of almost a factor of two by burying the guide below the surface (Findakly, Garmire, Appl. Phys. Lett. 37, 856 (1980). This can be accomplished by following the KNO_3 ion exchange with a $NaNO_3$ ion exchange step to decrease the refractive index at the surface relative to the waveguide (high K concentration layer). We thus expect that with further development, losses the order of 0.01 dB/cm at 1.3 μm will be achievable in S3* single-mode guides fabricated by potassium ion exchange. Losses of this order will be suitable for a commercially applicable inertial rotation sensor.

C. In-Plane Scatter

In addition to losses, we made comparative measurements of in-plane scatter, out-of-plane scatter and mode-mixing for various substrates and processes.

The technique of diffusion of silver films was studied because the losses in microscope slides were very low. We observed essentially no out-of-plane scatter and very little in-plane scatter. Because of the success with this process in microscope slides, we decided to apply it to optical glasses. We obtained substrates of soda-lime glass from Schott, S-3, and of phosphate glass, S-8000.

There was no out-of-plane scatter in the S-3 glass; indeed, the streak was invisible. Although the measured overall losses in S-8000 were lower, there was more out-of-plane scatter, presumably from the fact that the phosphate glass is more chemically reactive. Photographs of the prism-coupled m-lines show in-plane scatter, (Fig. VI-5), particularly for the S-3 glass. However, the photograph had to be over-exposed in order to detect

A. S3 glass; 400°C, 1 hour; 14 modes, waveguide 50 μm thick

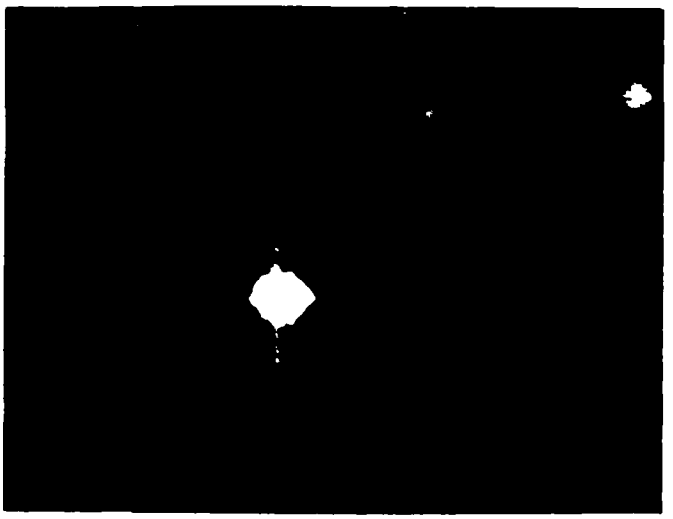

B. S8000 glass; 400°C, 1 hour; 8 modes, waveguide 28 μm thick

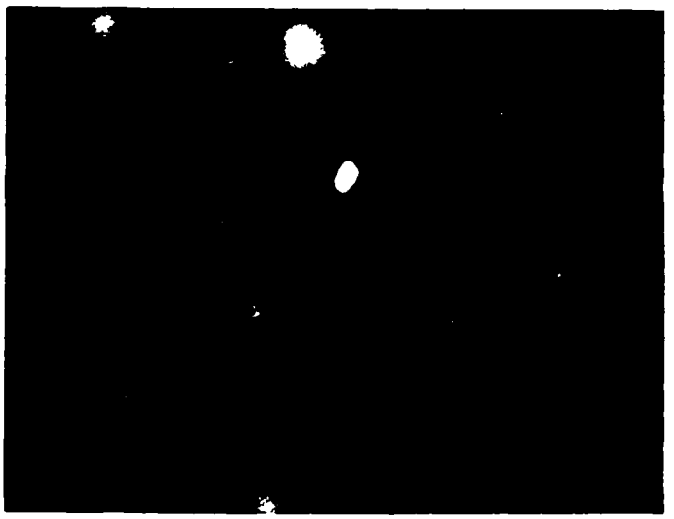

Figure VI-5. Far-field pattern of prism-coupled output from waveguides fabricated by thermal diffusion of a silver film. The plane of the waveguide is vertical. In-plane scatter is indicated by the weak vertical streak. Mode-mixing is indicated by the existence of more than one vertical line.

the weak in-plane scatter line. This sample of S3 was found to be lossy because of the presence of fining agents. We subsequently ordered new S3 without fining agents and observed lower loss than in S8000 glass, as described in the last section. This new S3 glass also had negligible in-plane scatter. However, it should be mentioned that these guides had very small refractive index increases and were 40 μm thick. It is thus not surprising that the scatter loss was small.

Since thermal diffusion of silver into S-3 glass did not provide a large enough index change for good quality single mode guides, we studied electro-thermal diffusion. We found that this process unfortunately introduced considerable in-plane scatter and mode-mixing. This is shown in Figure VI-6. In addition to scatter, the measured losses increased to 0.7 dB/cm for a waveguide of depth 3.5 μm. This seemed to indicate that silver as a diffusant was too lossy for the ring resonator. We therefore turned to potassium as a diffusant, introduced through ion exchange from a melt.

Using KNO_3 melts, the in-plane scatter was considerably smaller, as shown in Figure VI-7. However, lower order modes still have a small amount of in-plane scatter, and considerable intermode mixing. By comparison, the far-field outputs are shown for the KNO_3 melt in microscope slides, Figure VI-8. Direct comparison between Figures 7 and 8 are difficult because the exposures are different. However, it can be seen that there is very little in-plane scatter in microscope slides. We wanted to see whether the polishing process introduced in-plane scatter, so polished a microscope slide. The guided mode output distribution is shown in Figure VI-9. Some additional in-plane scatter is introduced by the polishing process, but since our techniques were not of optical quality this is not surprising.

In an attempt to identify the source of in-plane scatter, we coated the sample with low index liquid and studied waveguiding. We found that this had no impact on in-plane scatter, demonstrating that the scattering mechanism was due to sites within the waveguide, rather than on the surface. We did, however, find that the liquid on the surface increased the light coupled out the prism.

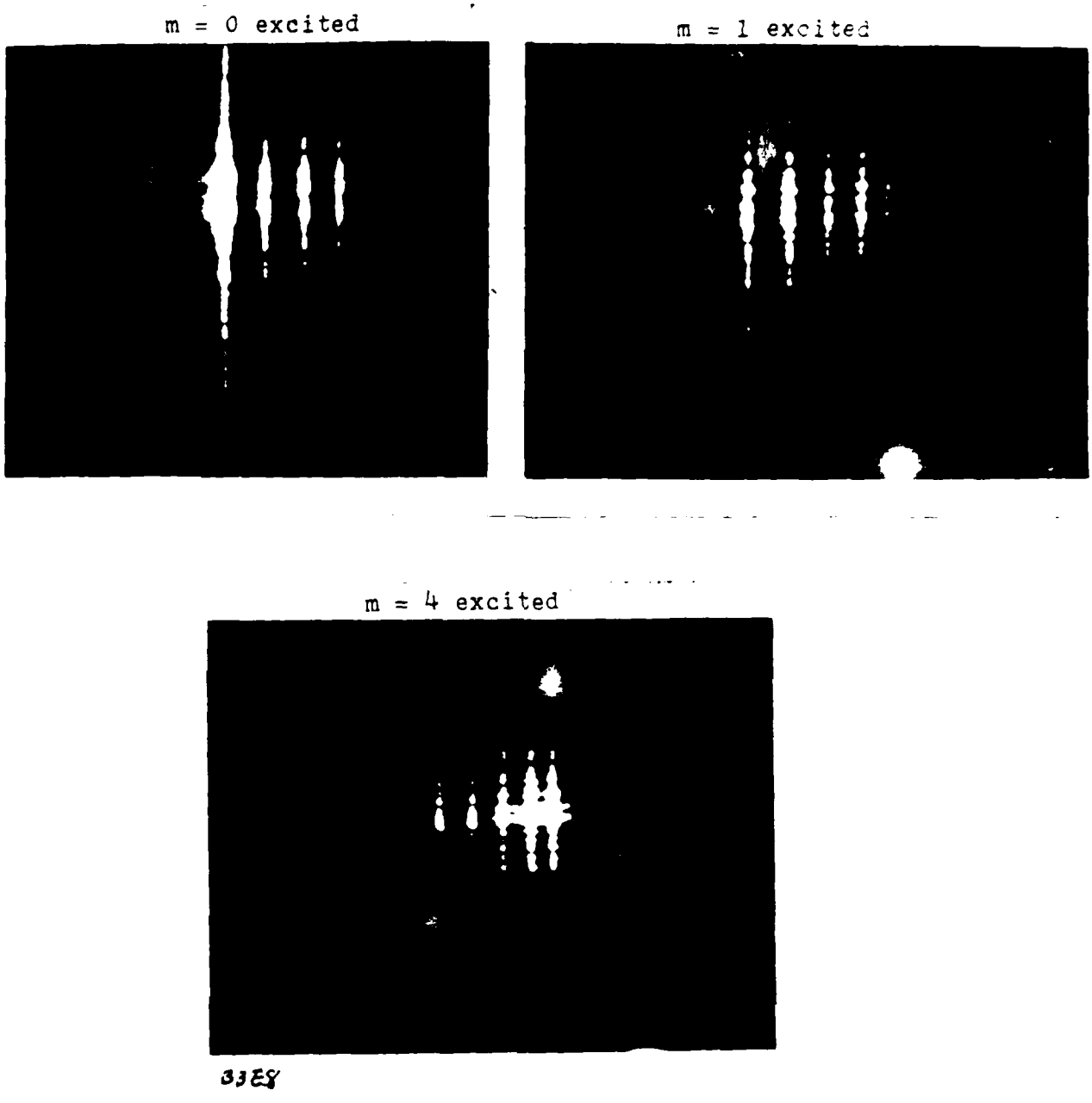

Figure VI-6. Far-field of prism output-coupled light from waveguide in S3* glass, fabricated by electric field-assisted diffusion of silver film (1000Å) using 20 V/mm for 15 minutes at 350°C. with post-diffusion anneal, 200°

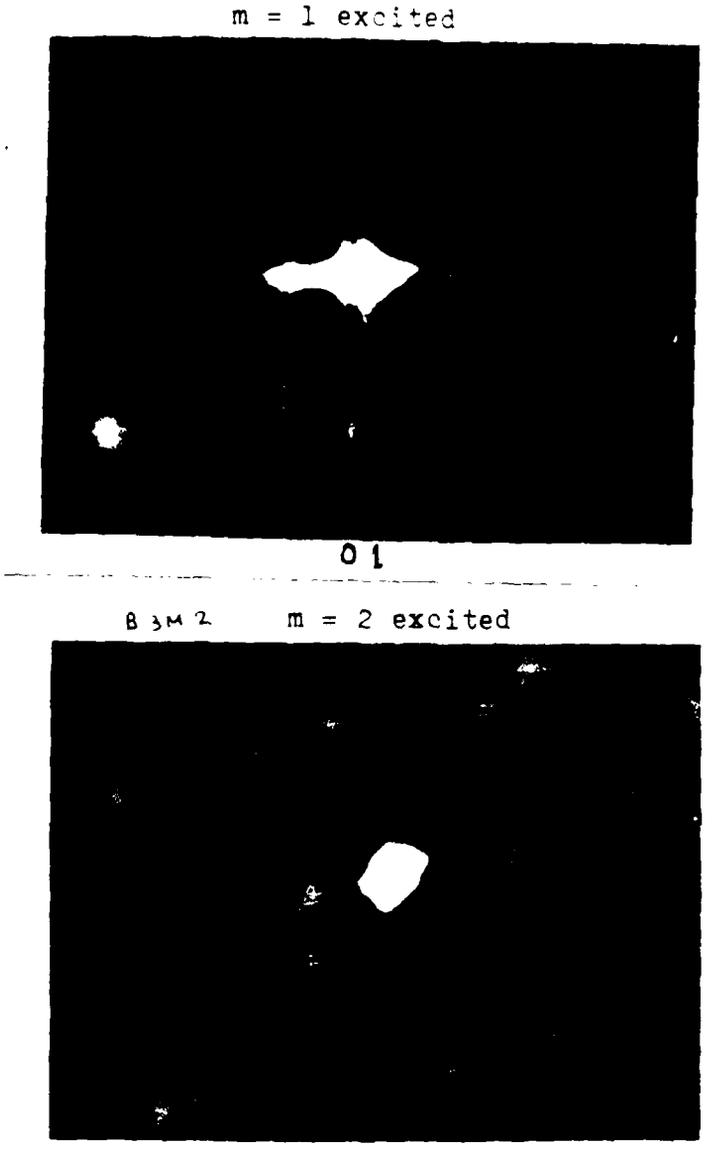

Figure VI-7. Far-field of prism-coupled output from ion-exchange waveguide in S3* glass, fabricated using KNO_3 at 350°C for 2 hours. Note the presence of ghost images (arrow). The intensity of this ghost depends on output prism coupling pressure, and is due to interference between the prism coupler and the waveguide.

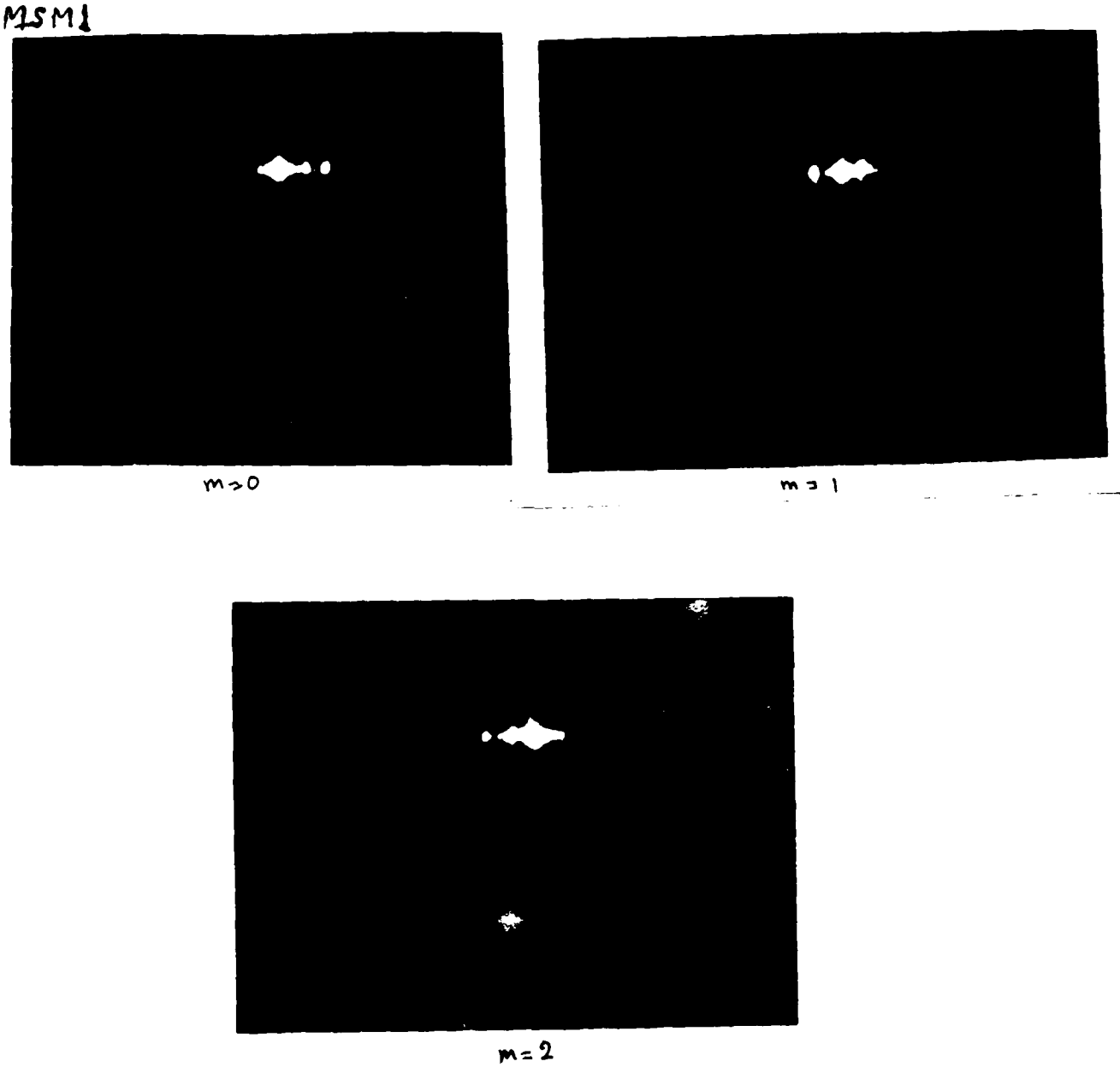

Figure VI-8. Far-field of light coupled with a prism from a waveguide fabricated by ion exchange in a microscope slide. A KNO_3 melt was used at 400°C for two hours. There were three modes with an effective depth of 9.6 μm.

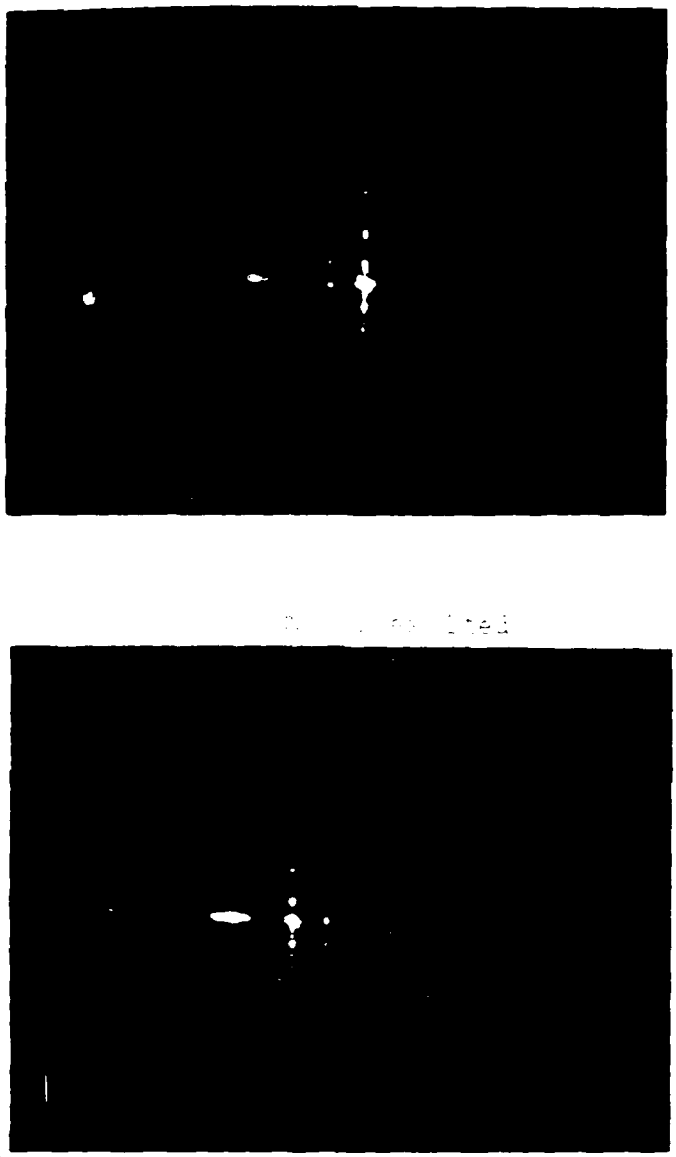

Figure VI-9. Far-field of light [illegible] prism [illegible] wavelength irradiated by [illegible] mirror [illegible]. The mirror [illegible] optical [illegible], and the resulting in-plane scatter [illegible]. The [illegible] for the second case.

One reason for the strong in-plane scatter with the optical glasses may be their polished surface. Although we determined that the surface was not the cause of in-plane scatter, the polishing process causes micro-cracks which may extend below the surface of the glass, causing in-plane scattering centers. Indeed, we obtained samples of S3 glass which had surfaces prepared by superpolishing, and the results are shown in Fig. VI-10. Very clearly, in this case, considerable in-plane scatter is caused by the polishing process. In this process an extremely flat surface is obtained by pressing during the polishing process and "smearing out" the surface. This leaves a highly damaged layer just below the surface which may be the source of the excess in plane scatter. We were not able definitively to prove that we measured the effect of microcracks. Clearly superpolish degrades the waveguide performance. Also, the enhanced scatter in field-assisted waveguides may be the result of stress-induced microcracks. More work needs to be done in this area to fully understand in-plane scatter.

It would be very useful to fabricate waveguides buried below the surface of the glass to determine whether or not the scatter is reduced. Our preliminary results on burying the guide below the surface reduced the loss by 0.8 dB/cm. That is, from 1.96 db/cm to 1.2 dB/cm. These experiments were preformed in microscope slides, which is the reason for the large total loss.

We experimented also with annealing the waveguides. However, we found that after anneal the scatter was no less, but the increased heating time introduced a new mode.

The results of this study were that KNO_3 is better than field-assisted diffusion of silver films in reducing the in-plane scatter. This is the process which we have decided upon for the ring resonator. Furthermore, for preliminary measurements with the ring, we decided to use Kodak lustra glass, flat glass prepared by a rolling process to avoid in-plane scatter.

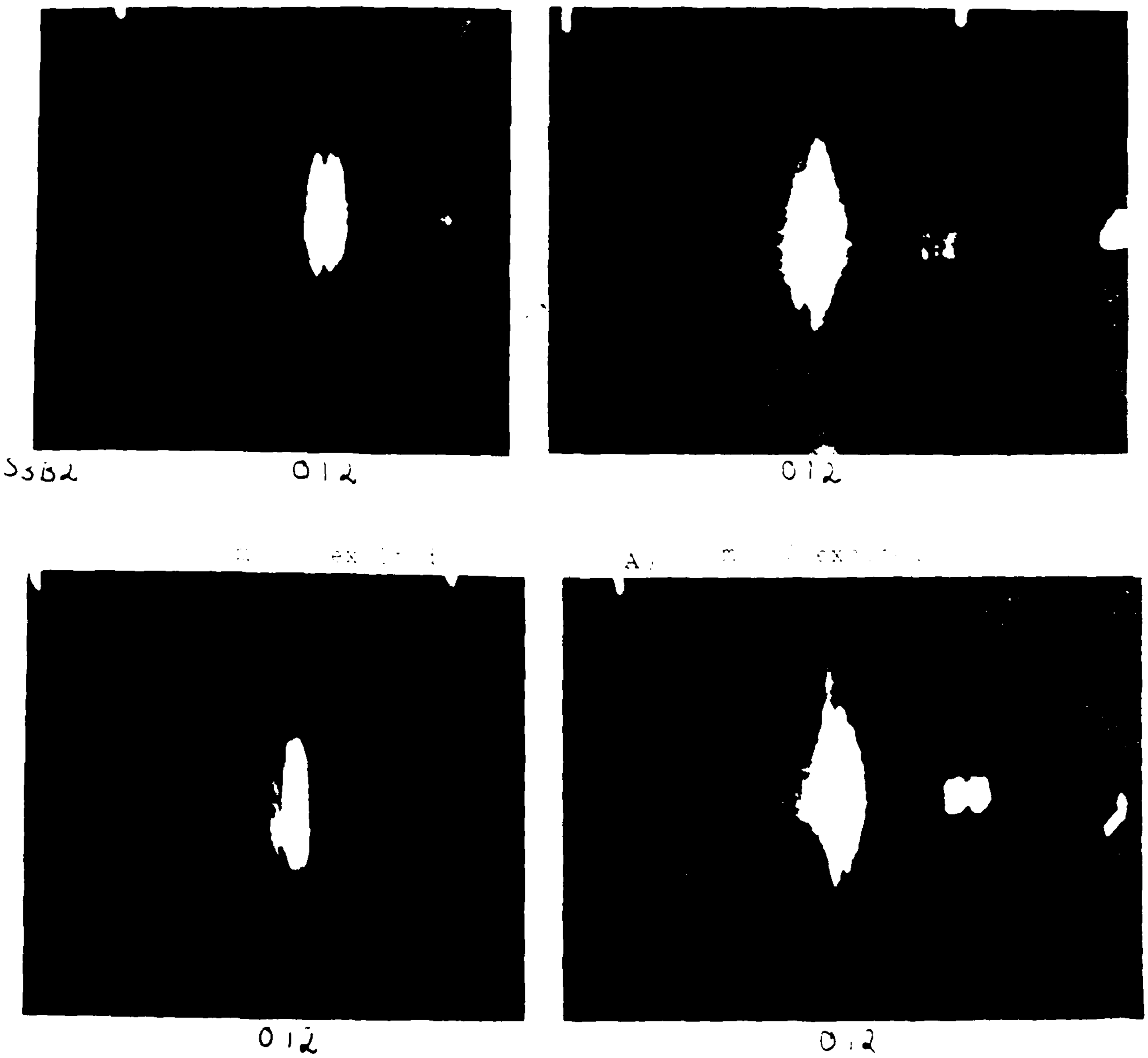

Figure VI-10. [illegible]ar-field of [illegible]utput prism-[illegible] [illegible]

VII. REFERENCES

H. Kogelnik, "Theory of Dielectric Waveguides" in Integrated Optics, ed. T. Tamir, Springer Verlag, NY, 1975 p. 24.

T. Findakly, C.L. Chen, Appl. Optics, 17, 769 (1978) "Optical Directional Couplers with Variable Spacing"

Wilson, Mueller, Garmire "Laser Writing of Masks for INtegrated Optical Circuits" IEEE Trans. Components, Hybrids and Manf. Techn. CHMT-5, 202 (1982)

T. Findakly, E. Garmire "Reduction and control of optical Waveguide Losses in Glass" Appl. Phys. Lett. 37, 855 (1980)

J. Haavisto and G. A. Pajer "Resonance Effects in Low Loss Ring Waveguides" Optics Lett. 5, 510 (1980)

R.G.Walker and C.D.W. Wilkinson, Appl. Opt. 22, 1029 (1983) "Integrated OPtical Ring REsonators made by Silver Ion Exchange in Glass"

R.G. Walker and C.D.W. Wilkinson, "Integrated OPtical waveguiding structures made by silver ion exchange in glass" Appl. Opt. 22, 1929 (1983)

T. Findakly, E. Garmire, H.T. Moon, Optics Lett. 4, 149 (1979) "Comparison of losses in imperfect surface-diffused and buried optical waveguides"

VIII. Information Dissemination

A. LIST OF PUBLICATIONS

T. Findakly, E. Garmire "Reduction and control of optical waveguide losses in glass" Appl. Phys. Lett. 37, 855 (1980)

K. Wilson, C. Mueller and E. Garmire "Laser writing of masks for integrated optical circuits" IEEE Trans. Components, Hybrids and Manf. Techn. CHMT-5, 202 (1982) Special issue of integrated optics fabrication technology.

T.N. Ding, E. Garmire "Measuring refractive index and thickness of thin films: a new technique" Appl. Optics 22, October 15(1983)

T.N.Ding, E. Garmire "Measurement of Thin film parameters using substrate excitation of leaky modes" Optics Letters, fall, 1983

"Integrated Optical circuits fabricated with laser-written masks" K.E.Wilson, C.T.Mueller, E. Garmire, Proc. SPIE vol 321 p. 5 (1982)

"Low loss Optical waveguide formation by field assisted solid state diffusion of metals in glass" K. Wilson, K. Cheng, E. Garmire, T. Findakly, Proc. SPIE Vol. 269 (1981) p. 148

"Ring Resonator and Quasi-waveguides as integrated optics devices for Measurements" E. Garmire, K. Honda, T.N.Ding, K.E.Wilson Proc. SPIE vol. 380, paper 96 (1983)

MANUSCRIPTS IN PREPARATION

K. Honda and E. Garmire "Depolarization in glass waveguides with non-straight walls" to be submitted to Applied Physics Letters

K. Honda and E. Garmire "Characteristics of an Integrated Optics Ring Resonator in Glass" to be submitted to Journal of Lightwave Technology

"Characteristics of diffused waveguides in Glass" K.E.Wilson, K. Honda and E. Garmire, to be submitted to Optics Communications

"Affect of Substrate on Losses in Glass Waveguides" K.E.Wilson and E. Garmire, to be submitted to Journal of Lightwave Technology

B. PERSONNEL WORKING ON THIS PROGRAM

Professor Elsa Garmire
K.E.Wilson , PhD
K. Honda
K. Cheng , PhD
T. N. Ding
T. Findakly, PhD

C. LIST OF PRESENTATIONS

T. Findakly, E. Garmire "Low Loss Optical waveguides fabricated by solid-state electro thermal diffusion of metals into glass" Presented at the Integrated Optics Conference, Nevada, 1980, January

"Properties of Low Loss Diffused optical waveguides in glass" T. Findakly, E. Garmire, Presented at the Topical Conference on Basic Optical Properties, National Bureau of Standarda, 1980, May

"Comparison of glass waveguide loss using different substrates" K.Wilson, E. Garmire, R.M. Silva, W.K.Stowell, Presented at the Optical Society of America Annual Meeting, 1981, October

"Optical Waveguides in glass by electro-thermal diffusion" T. Findakly, E. Garmire, Presented at the Annual Meeting of the American Vacuum Society, Anaheim, 1980

"Low loss Optical Waveguide Formation by field assisted solid= state diffusion of metals into glass" K. Wilson, K. Cheng, E. GArmire, T. Findakly, Presented at SPIE, Los Angeles, January 1981

"Integrated Optical Circuits fabricated with laser-written masks" K.E. Wilson, C.T.Mueller, E. Garmire, Presented at SPIE, Los Angeles, CA January 1982

"Ring resonator and quasi waveguides as integrated optics devices for measurements" E. Garmire, K. HOnda, T.N.Ding, K.E.Wilson Presented at SPIE, Washington, May, 1983

"Toward High Performance ring resonators in glass" E. Garmire, K. Honda, K. Wilson, Tobe presented at the Optical Society Annual Meeting, October, 1983

D. LIST OF CONTACTS WITH GOVERNMENT, INDUSTRY, UNIVERSITIES in the area of gyros and integrated optics

Wright/Patterson - Kent Stowell
RADC - Andrew Yang
Eglin AFB
National Bureau of Standards

National Science Foundation
grantee-user conference
in Optical Communications

Northrop -- Precision Products Division
McDonnell Douglas Udd
Lear Siegler - Gubbins
TRW Research Center
JPL
USC Industrial Associates
Batelle Laboratories
Kodak
Dupont
Honeywell

Stanford
M.I.T.
Berkeley U.C.
Irvine U.C.
SanDiego - U.C.

Reduction and control of optical waveguide losses in glass

T. Findakly and E. Garmire

Center for Laser Studies, University of Southern California, University Park, Los Angeles, California 90007

(Received 26 March 1980; accepted for publication 7 August 1980)

Reproducible waveguides were obtained by diffusion of silver films both with and without an applied electric field. Measurements of the mode, wavelength, and thickness dependences of the loss permit us to identify loss contributions from both the diffusant and also from surface roughness. Reduction of loss was achieved both by burying the waveguide below the surface of the substrate and also by performing measurements in the near infrared.

PACS numbers: 42.82. + n, 42.80.Lt

Glass optical waveguides are attractive candidates for passive integrated optical circuits which required low-loss, low-cross-talk waveguides and utilize low-cost substrates and simple processing techniques. These applications range from highly multimode buried guides for use with graded-index fibers to reproducible single-mode guides with very low loss. Most glass waveguides studied to date have been fabricated with ion exchange from molten salts of silver nitrate.[1] We found unreproducibility and relatively high loss using this process, and therefore have investigated using an oxidized silver film rather than a melt as a source for the exchange. We have fabricated waveguides both with and without an electric field applied during the diffusion.

We have observed much lower loss, better reproducibility, and less degradation with time than was obtained using molten salts. We have made measurements of waveguide loss as a function of mode number, waveguide thickness, and wavelength which have made it possible to obtain definitive information about the mechanisms of loss. Finally, by using the electric field to drive the silver ions below the surface of the glass/air interface, we have buried the waveguide, thereby reducing the loss due to surface roughness.[2] The initial results indicate as much as 0.8 dB/cm reduction in loss by burying the waveguide.

Silver films a few hundred angstroms thick were vacuum deposited onto soda lime silicate glass microscope slides. We report first on diffusions performed without an applied electric field. We observed waveguides of small index change (0.001) with thicknesses from several microns to several tens od microns, depending on diffusion time (a few minutes to a few hours) and temperature (the thickest waveguides were achieved at 500 °C). The index increase was much smaller than we observed in molten-salt ion exchange experiments (0.09), in marked contrast to the results of Chartier *et al.*[3] who reported that silver films and silver nitrate melts apparently gave the same index profiles. They reported a seven-mode waveguide diffused from a silver film at 250 °C for two hours, while we were unable to create even a single mode after diffusion for four hours at that temperature.

Loss measurements at 0.633 μm were made on these waveguides by proving the decrease in light scattered out of the waveguide along the propagation direction. Typical values of the loss as a function of waveguide thickness are shown in Fig. 1. These numbers are comparable to the best results reported for ion exchange from the melt.[4] The decrease in loss with increasing waveguide thickness is consistent with models for loss which depend either on surface roughness or on the silver concentration and therefore do not offer information as to the loss mechanism. However, the data indicate that meaningful loss measurements must include waveguide dimensions, since thicker waveguides always have lower loss.

To increase the refractive index in the waveguides, we applied an electric field to assist in the diffusion process. The electrodiffusion was carried out in air at temperatures in the range 300–350 °C, with an electric field of up to 100 V/mm applied for periods ranging from a few minutes to one hour. The ionic current density, ranging from a few microamperes to a few milliamperes per square centimeter, was monitored throughout.

Electrodiffused waveguides had index increases of up to 0.025, depending on applied field (in contrast to the results reported in Ref. 3). The index increase, guide thickness, and number of modes were easily controlled through varying the diffusion time, temperature, and applied electric field. Mode dispersion measurements were performed with prism coupling and the resulting index profile was determined from the effective indices of the guided modes using the usual WKB analysis. Typical index profiles are shown in Fig. 2.

The waveguides represented by curves a and b in Fig. 2 were fabricated using gold films as electrodes. Single-mode waveguides were easily obtained in this fashion using diffusion times of less than five minutes at 350 °C and 50 V/mm applied field. For highly multimode guides, however, with numerical aperatures approaching those of fibers, it was found that the cathode deteriorated with time (due to accumulation of sodium metal). Thus, to obtain thick waveguides as those shown in curves c and d, we introduce a molten

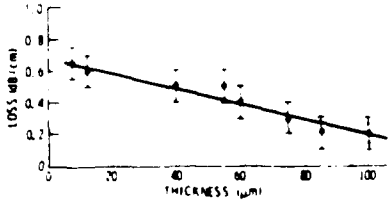

FIG. 1. Thickness-dependent losses in silver-film-diffused glass waveguides

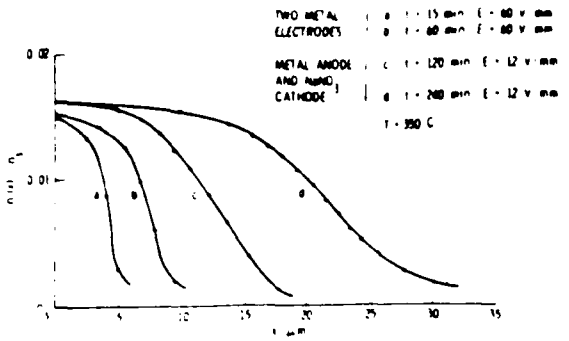

FIG 2 Index profile of electric-field-assisted silver-film-diffused glass waveguides

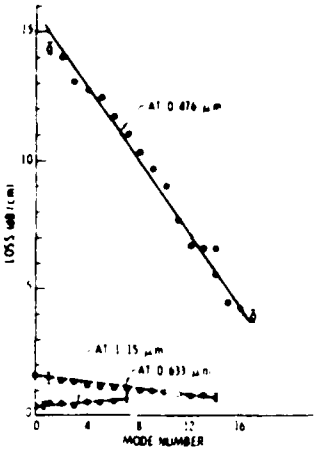

FIG 3 Mode-dependent losses in electric-field-assisted silver-diffused waveguides at 0.476-, 0.633-, and 1.15-μ wavelengths

sodium nitrate cathode. Required process times and applied fields we much smaller

Losses in these electrodiffused waveguides (measured at 0.633 μm) were typically the order of 1.5 dB/cm, higher than that measured in the low-index guides fabricated without an electric field. However, these losses were still much lower than those for guides of the same dimensions fabricated by ion exchange. Furthermore, waveguides fabricated in optical-quality glass had much higher losses than any reported here, owing to the additional presence of reducing agents in those glasses [5]

Information about the loss mechanism is determined by studying the mode dependence of the loss. Typical results are shown in Fig. 3, which shows the loss in the same waveguide at three different wavelengths. Losses originating from diffused silver are lower for higher-order modes since the latter have deeper optical penetration and accordingly encounter less silver. This dependence is demonstrated by measurement of waveguide loss at 0.476 μm, where the silver causes a large absorption loss. It is important to notice that the mode dependence of the loss at 1.14 μm is thereverse of that in the blue. This indicates that at near-infrared wavelengths, the predominant loss mechanism is surface roughness apparently on the order of 0.5 dB/cm. At 0.63 μm the two loss mechanisms are more or less comparable.

To avoid losses due to surface roughness, it is necessary to bury the waveguide below the surface. We fabricated buried waveguides by following electrodiffusion with a second electrodiffusion in the absence of a silver source. We observed a reduction in loss from 1.96 to 1.2 dB/cm for the lowest-order mode at 0.63 μm, with similar results for the other modes. As proof that the waveguide was buried, a substantial reduction in the coupling efficiency of a prism was observed, although the end-fire coupling remained effective. The reduction of almost 0.8 dB/cm by burying the guide at 0.63 μm is significant as a means of reducing the surface scattering component of the total loss and predicts very low-loss operation in the near infrared, where the volume loss is low.

In summary, we have decribed integrated optical glass waveguides formed by electrodiffusion of silver films. This technique proves to be eminently suitable for processing low-loss waveguides. We have demonstrated that these wavelengths have the capability of guiding single mode with losses well below 0.1 dB/cm at 1.15 μm, when the guide is buried below the surface.

The authors appreciate the skillful technique assistance of Ray Owen in sample preparation. This work was sponsored by AFOSR.

[1]See, for example, G. Chartier, P. Collier, A. Guez, P. Jaussaud, and Y. Won, Appl. Opt. 19, 1092 (1980); G. Stewart, C. A. Millar, P. J. R. Laybourn, C. D. W. Wilkinson, and R. M. DeLaRue, J. Quantum Electron. QE-13, 192 (1977).
[2]T. Findakly and E. Garmire, Opt. Lett. 4, 149 (1979).
[3]G. Chartier, P. Jaussaud, A. D. de Oliveira, and O. Parriaux, Electron. Lett. 14, 132 (1978).
[4]T. Giallorenzi, E. West, R. Kirk, R. Ginther, and R. Andrews, Appl. Opt. 12, 1240 (1973).
[5]G. E. Rindone and W. A. Weyl, J. Am. Ceram. Soc. 33, 91 (1950).

IX.B, 80

Laser Writing of Masks for Integrated Optical Circuits

KEITH E. WILSON, CRAIG T. MUELLER, MEMBER, IEEE, AND ELSA M. GARMIRE, FELLOW IEEE

Abstract—Masks for integrated optics applications have been fabricated using a focused Argon laser beam to expose a photoresist-coated gold-chrome plate. Curved and straight line masks were written using a combination of precision motor-driven rotational and translational stages to move the coated plate under the focused laser beam. By varying the laser power and/or writing speed, directional coupler masks have been made 3-μm wide separated by as little as 1 μm. From the results it is shown that narrow lines several centimeters long with better than 1000 Å edge roughness can be obtained by this fabrication technique.

GUIDED WAVE DEVICES, unlike conventional electronic devices, often require small dimensions on the order of microns in one direction and large dimensions on the order of centimeters in the perpendicular direction. Conventional photolithographic techniques such as electron beam writing and pattern generation methods have been shown to produce the high quality masking structures (200 Å edge roughness) [1] which are required in integrated optics. However, these techniques require some sort of "step, align, and repeat" procedure, often causing abrupt irregularities. In addition to the long lead time to delivery, these masks are expensive and fabrication of complex designs can rapidly deplete the resources of a modest research grant. The research scientist must therefore either deal with simple structures or find an alternative means of fabrication. Laser writing offers such an alternative.

The idea of using a laser beam to expose photoresist patterns a few microns wide and several centimeters long has been around for several years. Becker *et al.*[2], in their "Focused laser lithographic system," used an argon laser beam to directly expose a photoresist coated substrate and demonstrated that this technique is suitable for coating lift-off processes. We have used laser writing to expose commercially available photoresist-coated chromium masks and generated patterns suitable for contact printing. By also including a motor-driven rotational stage, we have generated arcs and complete ring patterns with less than 0.1 μm residual edge roughness. Such masks are suitable for fabricating variable spacing directional couplers and ring interferometers. By writing the patterns directly onto a mask we have avoided the difficulties of realigning the system to accommodate substrates of different thicknesses.

We have been exploring the possibilities of laser writing of masks for applications which require long waveguides only a few microns wide. In particular, we are working on the development of a ring interferometer in glass, consisting of a ring waveguide 10-cm diameter and directional couplers for input and output coupling. The apparatus shown in Fig. 1 has been designed for this purpose.

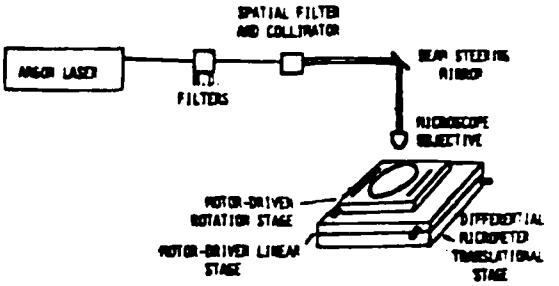

Fig. 1. Experimental arrangement for laser writing of masks.

A combination of neutral density filters and polarizers were used to vary the laser power, and the patterns were written by using precision motor-driven translational and rotational stages to move the mask under the focused laser beam. By changing the distance from the axis of rotation to the position of the focused beam, we were able to vary the radius of rings and the curvature of circular sections. Directional couplers were fabricated by laterally translating the mask a few micrometers before writing the next pattern. The lateral motion of the stage was monitored using a Twyman-Green interferometer, one arm of which consisted of a reflector mounted on the translational stage. By recording the motion of the interference fringes resulting from the change in optical path length, we were able to determine accurately the center to center separation between two adjacent lines. Vibrational isolation was achieved by mounting the entire system on an air suspension optical table.

Masks suitable for contact printing were fabricated using a standard gold-chrome mask coated with a thin layer (5000 Å) of positive photoresist (AZ 1350J). Although the optimum operating range for this resist is around 350 nm, we have found it to be sufficiently sensitive at the short Argon laser wavelengths (4545 Å and 4579 Å) to obtain good patterns when operating at microwatt laser powers. Using the 4545 Å Argon wavelength, we have written lines as small as 2.5-μm wide which is on the order of the diffraction limited spot size. In this paper we demonstrate some of the structures which laser writing can produce and indicate some of the fabrication limits of the process.

Typical laser powers for laser writing range from 8 μW to 0.5 mW with writing speeds varying from 0.3 to 3 mm/s. Making use of the laser beam's Gaussian intensity profile to control the linewidth, lines ranging in width from 2 μm to 24 μm have been produced by adjusting both the laser power and translation rate. Alternatively, the linewidth can be

Manuscript received August 14, 1981; revised November 18, 1981. This work was supported by the Air Force Office of Scientific Research.

The authors are with the Center for Laser Studies, University of Southern California, University Park, Los Angeles, CA 90007.

0148-6411/82/0600-0202$00.75 © 1982 IEEE

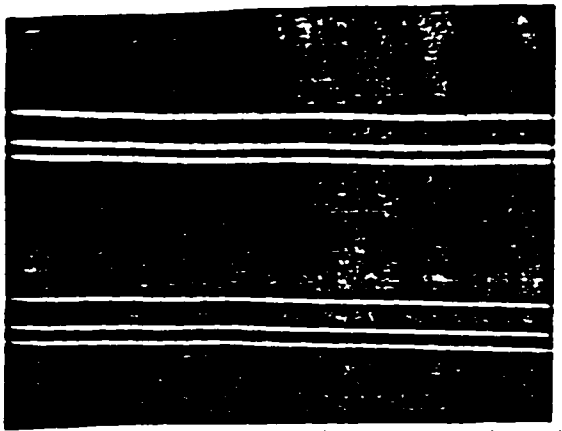

Fig. 2. 204.8× magnification of mask for parallel lines fabricated by laser writing. Lines 4-μm (lower group) and 7-μm (upper group) wide were written using 40 μW and 80 μW of laser power, respectively.

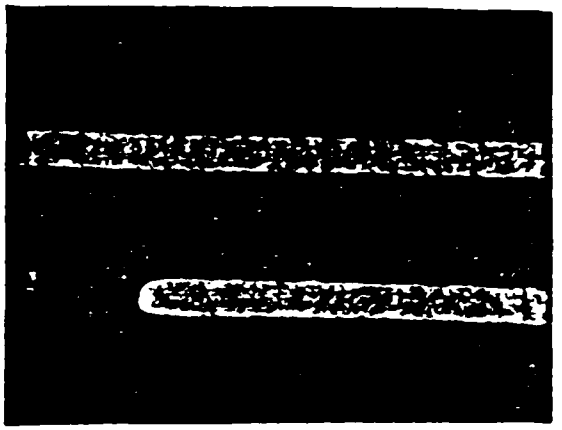

Fig. 3. 960× magnification of 6-μm wide lines showing a 6-μm period in edge roughness.

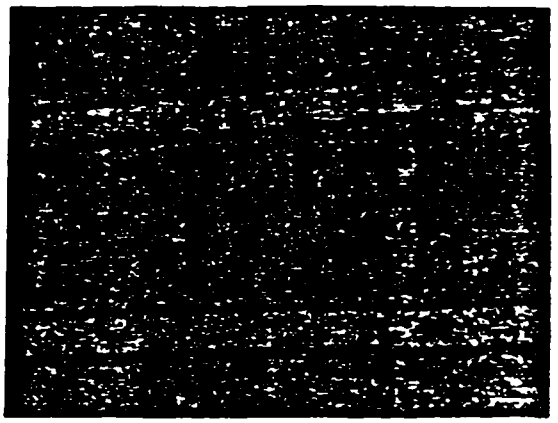

Fig. 4. Pre-etch photographs of lines written with the rotational stage (top) and the translational stage (bottom). Notice that there is no wobble present in the top trace even at this 960× magnification.

varied by defocusing the laser beam or by using a different microscope objective. The two parameters which determine the precision to which the writing stage must be aligned are the focused spot size and the depth of focus. For a Gaussian beam, the minimum spot size is given by $1.3\,\lambda f/d$ where λ is the wavelength, f is the focal length of the objective lens, and d is the beam diameter [3]. For a 2-mm beam diameter and a 20 × microscope objective, the calculated minimum spot size (separation of $1/e^2$ power points) is 2.3 μm. With this microscope objective and a translational speed of 0.3 mm/s, 4-μm and 7-μm wide lines have been written at laser powers of 40 μW and 80 μW, respectively (Fig. 2). The depth of focus for a Gaussian beam is given by $\pm 2.5\,\lambda (f/d)^2$. The calculated depth of focus for our arrangement was ± 18 μm. Thus the focused spot size did not change significantly within the 0.5-μm thick photoresist layer. However to obtain lines of uniform width over long distances, optical alignment of the translational stage over the length of the beam travel is crucial. This was achieved by ensuring that reflected and incident beams remained collinear over the length of the travel of the stage. With this alignment procedure, we were able to write lines 4-μm wide over a 6-cm length.

A typical line drawn by laser writing is shown in Fig. 3. Notice that the edges are sharp. However there is approximately 1000 Å residual edge roughness of about 6-μm periodicity along the length of the line. Possible mechanisms for the residual edge roughness are fluctuations in laser power, deviations of the translation stage, vibrations in the system and photoresist processing limitations. To determine the cause of the edge roughness, we compared the lines drawn by using the rotational and translational stages. The arcs written with the rotational stage were of very high quality with no edge roughness measurable at 1200X magnification. An example is shown in the top channel of Fig. 4. In comparison the line drawn using the translational stage (bottom channel in Fig. 4) does exhibit 0.1-μm residual edge roughness. This indicated that random variations such as fluctuations in laser power and system vibrations were not the cause of the observed edge roughness but instead it was due to a slight wobble in the translation stage. In addition to the edge roughness, the edge of the bottom lines show the effects of incomplete development. However, edge sharpness can be enhanced by optimizing the exposure so that the photoresist channel edge occurs at the half power point of the focused Gaussian beam.

Directional couplers can be made by combining an arc and a straight line (or two arcs), separated by a small distance. For this purpose we wrote arcs of 40-cm radius of curvature, of width 3 μm and length 5 cm. We also wrote a ring waveguide, 7 cm in diameter with a linewidth of 15 μm. This ring will form the basis for a ring interferometer [4]. To further explore the potential of laser writing for directional couplers, we wrote several lines using the translation stage and varying the separation between the lines. One such pattern is shown in Fig. 5. The lines are 2.5-μm wide with 1.5-μm edge to edge separation. For this exposure, the separation between these lines was controlled by a differential screw translator which had a resolution of 0.125 μm. The results obtained using the differential translator are similar to those obtained with the Twyman–Green interferometer. Other structures written by laser writing are the crossed and Y power splitters shown in Figs. 6(a) and 6(b).

Fig. 5. 960× magnification of directional coupler mask written by laser writing. Lines are 2.5-μm wide and separated by 1.5 μm.

We found it difficult to align our setup sufficiently and accurately to write both an arc and a straight line separated by the required spacing for a directional coupler. More typically, the two lines would intersect. For this reason we have found it most convenient to write a master arc and straight line, and to contact print both onto another mask, carefully adjusting the spacing under a microscope.

We have fabricated both glass and $LiNbO_3$ waveguides, single and multimode, using these masks. We have not made careful comparison of waveguides made with these masks and those made by electronic-beam written masks, but are confident that the laser-written masks compare favorably. We are now using laser-written masks for all our optical circuits.

In conclusion, we have demonstrated some of the capabilities of laser writing as a tool for fabricating masks for integrated optics circuits. We believe that the potential advantages of this technique are sufficient to make it a viable option to existing methods. One possible extension of the technique would be to use a computer controlled X-Y stage to fabricate arbitrary mask structures. In the meantime, we have found the combination of one translation and one rotation stage gives enough flexibility for several applications.

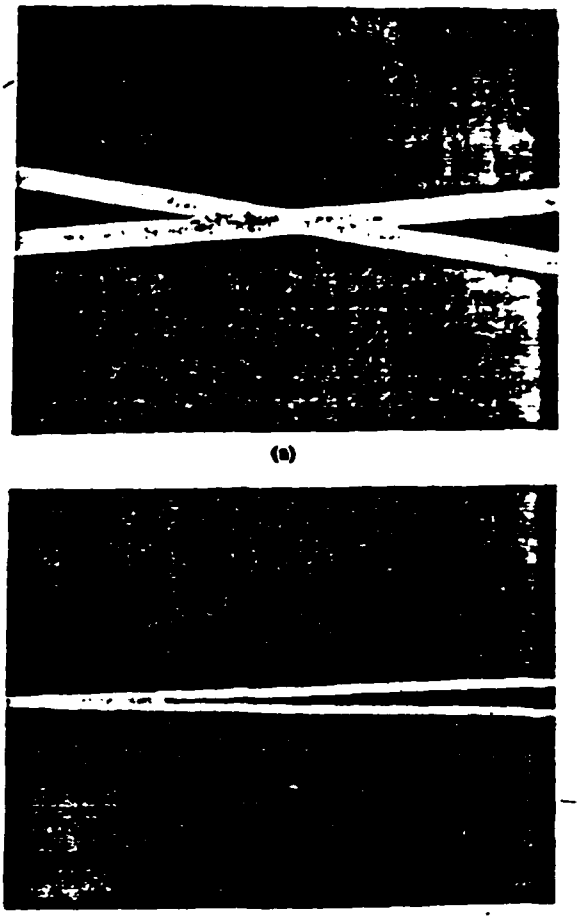

Fig. 6. Masks for power splitters under 204.8× magnification. (a) Crossed power splitters. Lines are 16-μm wide. (b) Y power splitters. Lines are 6-μm and 8-μm wide.

REFERENCES

[1] M. Barnoski, *Introduction to Integrated Optics*. New York: Plenum, 1974, p. 178.
[2] R. A. Becker *et al.* "Focused laser lithographic system," *Appl. Opt.*, vol. 17, p. 1069, 1977.
[3] A. Yariv, *Quantum Electronics*. New York: Wiley, 1975, p. 117.
[4] J. Haavisto and G. A. Pajer "Resonance effects in low-loss ring waveguides," *Optics Lett.*, vol. 5, p. 510, 1980.